PHYSICAL REVIEW B VOLUME 27, NUMBER 12 15 JUNE 1983

Self-consistent impurity calculations in the atomic-spheres approximation

O. Gunnarsson, O. Jepsen, and O. K. Andersen
Max-Planck-Institut für Festkörperforschung, Heisenbergstrasse 1, D-7000 Stuttgart 80, Federal Republic of Germany
(Received 17 January 1983)

We have developed a method for calculating self-consistently the electronic structure around an impurity atom, or an impurity cluster, in a crystalline host. Our method is a Green-function matrix technique based on the linear muffin-tin orbital method in the atomic-spheres approximation. The calculation of the host Green function is extremely efficient and involves diagonalization of a small Hamiltonian matrix for the band structure and subsequent Hilbert transforms. The method is tested for the calculation of one-electron spectra and total energies on systems for which (essentially) exact solutions are known: the Hulthén potential, a free H atom, a H atom in jellium, and a Li atom in jellium. The accuracy is better and the computational speed significantly higher than that obtained with the standard Korringa-Kohn-Rostoker Green-function technique.

I. INTRODUCTION

It has recently become possible to perform *ab initio* self-consistent electronic structure calculations for deep impurities in semiconductors[1,2] and for impurities in metals.[3] The perturbation from such impurities is stronger and more localized than that from shallow impurities and this makes the usual effective-mass approximation invalid. The perturbation is, on the other hand, too extended to be treated as atomiclike. This intermediate character thus requires more involved calculations.

Semiempirical tight-binding methods have been successful[4] in explaining certain chemical trends for deep impurities in semiconductors. We believe that a similar formalism can be obtained from the *ab initio* linear muffin-tin orbital method in the atomic-spheres approximation (LMTO-ASA).[5–7] For closely packed metals this method has been demonstrated to combine efficiency and physical transparency with fairly high accuracy.[8,9] Its potential parameters and structure constants have been tabulated for all elemental metals. In this paper we adopt this method to *ab initio* calculations for localized impurities.

Of the existing *ab initio* calculations for impurities, some have been based on a cluster approach in which the perfect solid and the impurity atom are replaced by a finite cluster,[10] which may be repeated periodically.[11] Most calculations, however, treat the proper infinite system using a Green-function method. An advantage of this is that the problem separates into two parts. First, the Green function G^0 of the perfect solid is calculated using one of the band-structure methods developed for infinite crystals. Then the Green function G for the solid with the impurity is calculated by solving Dyson's equation $G=G^0+G^0\Delta V G$ with the perturbation ΔV from the impurity. Dyson's equation is usually turned into a matrix equation in which the range of ΔV determines the size of the matrix. This method is very convenient for the problem we have in mind. Here ΔV is large only in a small region of space while the wave functions and the local densities of states are perturbed over a larger region.

The Green-function method was first used in this context by Koster and Slater.[12] It was further developed by Callaway[13] and subsequently found numerous applications.[14,15] Recently, in particular, three groups have used this method. Bernholc, Pantelides, and co-workers[1] as well as Baraff, Schlüter, and their co-workers[2] have developed methods in which the wave functions are expressed as linear combinations of Gaussian orbitals. These schemes have been successfully applied to deep impurities with s and p electrons, and it was demonstrated that for these systems the calculations can be performed without any substantial approximation for the potential. Zeller, Dederichs, and co-workers[3] have treated impurities in (transition) metals using the muffin-tin (MT) approximation for the potential and the Korringa-Kohn-Rostoker (KKR) scattering formalism to solve Schrödinger's equation.

In the KKR formalism the wave functions are expressed in terms of the partial waves $\phi_{RL}(E,r)$ which satisfy Schrödinger's differential equation

 ©1983 The American Physical Society

$$[-\nabla^2+v_R(r)-E]\phi_{Rlm}(E,\vec{r})=0\ . \tag{1.1}$$

with $v_R(r)$ being the spherically symmetric potential inside the MT sphere at site R and constant outside. In (1.1) and throughout this paper we use atomic rydberg units and let $L=l,m$ denote the quantum numbers of angular momentum. The partial waves at energy E are used to construct the Green function $G(E)$. This approach has the advantage of providing an exact solution for the MT potential, regardless of its strength. Also for non-MT potentials the partial waves, in the form of so-called muffin-tin orbitals (MTO's), are well suited to represent the wave functions. This has most clearly been demonstrated in LMTO calculations for small molecules.[16]

Gaussian orbitals, on the other hand, are often used with some computational advantage but they are not as well suited for an expansion of the wave function as the partial waves, and at least twice as many basis functions are needed for the same accuracy. Moreover, in the Gaussian scheme the wave functions of the system with an impurity are usually expressed in terms of the wave functions of the pure system. If the impurity atom is drastically different from the host this means that very high-lying states of the unperturbed system must be taken into account. Recently, methods for dealing with this inconvenience have been proposed.[17]

In a formalism based on Eq. (1.1), there are no particular difficulties in treating impurities that are very different from the host atoms, since the partial waves may be calculated in the presence of the impurity potential. Although the KKR formalism takes advantage of this fact, there is nevertheless no natural cutoff in the number of bands included in the calculation of $\mathrm{Re}G^0(E)$. The reason for this is that (1) the KKR structure constants and (2) the partial waves depend on energy.

The structure constants are essentially the matrix elements of the free-electron Green function G^{00}, defined through

$$(\nabla^2+\kappa^2)G^{00}(\vec{r}-\vec{r}\,';\kappa^2)=\delta(\vec{r}-\vec{r}\,')\ . \tag{1.2}$$

In terms of these the Green function for the unperturbed crystal, defined through

$$[\nabla^2+E-V(\vec{r})]G^0(\vec{r},\vec{r}\,';E)=\delta(\vec{r}-\vec{r}\,')\ , \tag{1.3}$$

is given by a Dyson equation with the perturbation $E-V(\vec{r})-\kappa^2$. In the KKR method, where $V(\vec{r})$ is a MT potential with the constant value V_{MTZ} between the spheres, the choice

$$\kappa^2=E-V_{\mathrm{MTZ}} \tag{1.4}$$

is made in order to ensure free propagation between the spheres. This makes the KKR structure constants depend on energy.

We shall avoid this energy dependence by using the ASA.[5] The ASA consists of the choice

$$\kappa^2=0 \tag{1.5}$$

and of the approximation that the integral over all space

$$\int G^{00}(\vec{r}-\vec{r}\,';0)[E-V(\vec{r}\,')]G^0(\vec{r}\,',\vec{r}\,'';E)d^3r'$$

equals the sum of integrals over "space-filling" atomic spheres whose overlap is neglected and whose potentials are spherically symmetric. For closely packed materials (e.g., metals), it is suitable to use spheres centered on the atoms while for open structures (e.g., semiconductors), additional spheres cover the holes in the structure.[18] As a consequence of the choice (1.5) the ASA structure constants are independent of energy.

The remaining energy dependence is that of the partial waves (1.1). We shall approximate this energy dependence by the first two terms

$$\phi(E,r)=\phi(E_\nu,r)+(E-E_\nu)\dot{\phi}(E_\nu,r)+o(E-E_\nu)\ , \tag{1.6}$$

of the Taylor expansion about some arbitrary energy E_ν.

As a result of the ASA (1.5) and the linearization (1.6) it is now possible to relate $G^0(E)$ to an ordinary linear eigenvalue problem of low dimension. The corresponding Hamiltonian[7] is exceedingly simple and its nine s, p, and d bands (per atom) have upper and lower bounds. The calculation of $G^0(E)$ therefore proceeds much faster than with the KKR method. Moreover, the Hamiltonian is physically meaningful and it yields energy bands correct to second order in $E-E_\nu$.

Koenig, Léonard, and Daniel[14] recently developed a LMTO-ASA method for impurities by taking the $\kappa^2\to 0$ limit of the KKR formalism.[3] Although derived in a different way, our results agree with theirs, as they must. However, Koenig *et al.* did not discover the above-mentioned Hamiltonian way of expressing G^0 but rather calculated the energy bands and Bloch functions with the standard LMTO-ASA procedure and then obtained $\mathrm{Re}G^0(E)$ in essentially the same way as with the KKR method.

We shall present our LMTO-ASA formalism for self-consistent impurity calculations in Sec. II. We also show how the total energy is conveniently calculated within the local approximation to the density-functional formalism.[19] In Sec. III we then test our method on different model systems for

which exact, or nearly exact, results are known. Our solution of Schrödinger's equation is tested on the so-called Hulthén potential and thereafter our self-consistent method is tested on the hydrogen atom, on a proton in jellium, and on lithium in jellium. The ASA results are found to be satisfactory, in general, and more accurate than the results obtained with the MT approximation in which perturbations in the interstitial region cannot be taken into account. The errors due to the energy linearization and the overlap of the atomic spheres are found to be small. The largest errors come from calculating the total energy with spherical charge densities. In Appendix A we derive and discuss expressions for the Green function $G(\vec{r},\vec{r}';E)$ valid for any value of κ^2. This illustrates the relation between the KKR and ASA methods and gives the LMTO-ASA formalism for a general (energy-independent) value of κ^2.

II. FORMALISM

In this section we reiterate how Schrödinger's equation for one electron is formulated in the ASA.[5–7,20] We define the atomic-spheres potential, the MTO, the potential functions $P_{Rl}(E)$, and the canonical structure constants $S_{Rlm,R'l'm'}$. We then derive the *secular equations* $[\underline{P}(E)-\underline{S}]\times[\underline{P}(E)]^{-1/2}\underline{B}=0$, whose solutions are the wave-function coefficients $B_{Rlm,j}$ and the one-electron energies E_j. These equations are particularly suited for treating the impurity problem via the Green-function technique because if we chose as the unperturbed system the perfect crystal with the Green-function matrix $\underline{g}^0(E)\equiv[\underline{P}^0(E)-\underline{S}]^{-1}$, then the perturbation $\underline{P}(E)-\underline{P}^0(E)$ only concerns the potential functions and is limited to the few diagonal elements corresponding to the impurity and the near-neighbor sites. The Green-function matrix for the crystal with the impurity $\underline{g}(E)=[\underline{P}(E)-\underline{S}]^{-1}$ may thus be found by solving the Dyson equations

$$\{\underline{1}+\underline{g}^0(E)[\underline{P}(E)-\underline{P}^0(E)]\}\underline{g}(E)=\underline{g}^0(E)\ . \tag{2.1a}$$

In order to see that these reduce to a *finite* set of linear inhomogeneous equations, we introduce the combined index $i=R,l,m$ and assume that there are N perturbed sites. In the perturbed region the index i runs over $M=N(l_{\max}+1)^2\approx 9N$ values. The matrix elements g_{ij}, where $1\le i\le M$ and $1\le j\le M$, are seen to be given by

$$\sum_{i=1}^{M}[\delta_{ki}+g^0_{ki}(P_i-P_i^0)]g_{ij}=g^0_{kj} \tag{2.1b}$$

for $1\le k\le M$. In (2.1b) we have dropped the argument E.

The Green-function matrix for the unperturbed crystal is, however, rather difficult to evaluate directly because of the nonlinear energy dependence of the potential functions. These may be approximated as follows[5]:

$$P(E)\approx\tilde{P}(E)=\frac{\Gamma}{V-E}+Q\ , \tag{2.2}$$

where V, Γ, and Q are so-called potential parameters. The approximations $\tilde{P}(E)$ are correct to second order in $E-E_\nu$, where E_ν is the (arbitrary) energy about which the potential functions are expanded. We show that the secular equations with $\tilde{P}(E)$ substituted for $P(E)$ may be transformed into ordinary *eigenvalue equations*, $(\underline{H}-E\underline{1})\underline{B}=0$, whose unperturbed Green-function matrix $\underline{\tilde{G}}^0(E)\equiv(E\underline{1}-\underline{H}^0)^{-1}$ may be obtained in the usual way from the eigenvalues and eigenvectors of $\underline{H}^0$ using projected densities of states and Hilbert transforms. Having obtained $\underline{\tilde{G}}^0(E)$ in this way, we may transform it into $\underline{\tilde{g}}^0(E)$, which is finally used in the Dyson equation (2.1) for $\underline{g}(E)$. Alternatively, we might have stayed in the $\underline{H}-E\underline{1}$ representation and thus solved the Dyson equation for $\underline{\tilde{G}}(E)$, but since the perturbation $\underline{H}-\underline{H}^0$ is not diagonal and is somewhat less localized around the impurity than $\underline{P}(E)-\underline{\tilde{P}}^0(E)$, this is less convenient. Besides, using the Dyson equation for $\underline{g}(E)$ allows us to use the correct potential functions (P rather than $\tilde{P}$) on the perturbed sites. In this way approximate potential functions are only being used outside the perturbed region.

Compared with the usual LMTO-ASA equations $(\underline{H}^{\rm LMTO}-E\underline{O}^{\rm LMTO})\underline{A}=0$, the eigenvalue equations $(\underline{H}-E\underline{1})\underline{B}=0$ are much simpler because $\underline{H}$ has the two-center form and the overlap matrix is the unit matrix.[7] The eigenvalues, but not the eigenvectors, of the usual LMTO-ASA equations are, however, slightly more accurate; they differ from the correct one-electron energies, as defined by $\det[\underline{P}(E)-\underline{S}]=0$, by terms of order higher than $(E-E_\nu)^3$, while the eigenvalues of $\underline{H}$ differ by terms of order higher than $(E-E_\nu)^2$.

The Hamiltonian matrix $H_{Rlm,R'l'm'}$ may be expressed in terms of the structure matrix $\underline{S}$ and the above-mentioned potential parameters V, Γ, and Q, which are diagonal in R,l,m as

$$\underline{H}=\underline{V}+\underline{\Gamma}^{1/2}(\underline{Q}-\underline{S})^{-1}\underline{\Gamma}^{1/2}\ , \tag{2.3}$$

which is simply the matrix generalization of the so-called scaling relation between canonical bands $\underline{S}$ and unhybridized energy bands.[5–7] In the matrix form (2.3), hybridization is included. A derivation of this simpler formulation of the LMTO method

was given in Ref. 7 in terms of the energy-independent, or $\phi,\dot{\phi}$-augmented, MTO's and their transformation into orthogonal orbitals. A derivation which is more straightforward and which allows the use of exact potential functions on the perturbed sites will be given below. At the end of this section we shall discuss the calculation of the total energy.

A. Secular equations and their Green function

We wish to solve the Schrödinger equation for an infinite system characterized by a one-electron potential of the atomic-sphere (AS) form. The AS potential is spherically symmetric inside spheres located at sites R and with radii s_R. The sites may be atomic sites and, in open structures, additional interstitial sites where the potential is usually repulsive. The AS potential may therefore be expressed as

$$V(\vec{r})=\sum_R \Theta(r_R/s_R)v_R(r_R)\ , \tag{2.4}$$

where the local coordinates are

$$\vec{r}_R=\vec{r}-\vec{R}\ , \tag{2.5}$$

and $\Theta(r_R/s_R)$ is a step function being unity inside a sphere of radius s_R and zero outside.

So far, the definition of the AS potential is identical to that of a MT potential; however, in the region between the spheres, the AS potential is assumed to be equal to the one-electron energy E, that is, the kinetic energy $E-V(\vec{r})$ is assumed to vanish. Moreover, the wave functions are normalized over the volume inside the spheres only and this means that the charge density between the spheres is neglected in the ASA. For these reasons we shall allow the spheres to have a slight overlap, such that the sum of their volumes fill space. For the fcc, bcc, and diamond lattices our construction leads to overlaps of up to about 15% for the radii (i.e., $s_R+s_{R'} \leq 1.15\,|\vec{R}-\vec{R}'|$).

Schrödinger's differential equation (1.1) separates inside a sphere so that its solutions may be taken as the partial waves

$$\phi_{RL}(E,\vec{r}_R)\equiv\phi_{Rl}(E,r_R)Y_L(\hat{r}_R)\ , \tag{2.6}$$

where Y_L is a real spherical harmonic, L is short for lm, and ϕ_{Rl} is the solution of the radial Schrödinger equation for the energy E and the potential $v_R(r_R)$. We shall assume that ϕ_{RL} is normalized to unity in its sphere, i.e., that

$$\int_0^{s_R}[\phi_{Rl}(E,r)]^2r^2dr=1\ . \tag{2.7}$$

Outside its sphere the partial wave is assumed to have zero kinetic energy, which means that it is a solution of Schrödinger's equation with the constant potential $v_R=E$ or, in other words, that it is a solution of the Laplace equation. We furthermore require that the partial wave is continuously differentiable, which leads to the form

$$\phi(E,r)=\phi(E,s)\left[\frac{D(E)+l+1}{2l+1}\left[\frac{r}{s}\right]^l+\frac{l-D(E)}{2l+1}\left[\frac{r}{s}\right]^{-l-1}\right] \tag{2.8}$$

for the tail ($r\geq s$) of the radial function. Here we have dropped the subscripts R and l. In (2.8), $D(E)$ is the logarithmic derivative of the radial wave function, i.e.,

$$D(E)=\left[\frac{\partial\ln\phi(E,r)}{\partial\ln r}\right]_{r=s}\ . \tag{2.9}$$

This is an ever-decreasing cotangentlike function of energy.

A wave function at energy E for the entire system may, if it exists, be expressed in the neighborhood of each site R as a one-center expansion

$$\psi(E,\vec{r})=\sum_L \phi_{RL}(E,\vec{r}_R)B_{RL}\ . \tag{2.10}$$

This is valid inside the sphere at $\vec{R}$ and between the spheres until r_R exceeds the distance to the nearest neighbor. The coefficients B are determined by the condition that the expansions around the various sites join continuously and differentiably onto one another. In order to express this matching condition analytically, it is convenient to define, in addition to the partial waves, the so-called MTO's (which in the present context ought to be named AS orbitals).

The MTO may be obtained from the partial wave simply by subtracting the part which diverges at infinity as r^l. The radial part of the MTO is therefore

$$\chi(E,r)=\phi(E,s)\times\begin{cases}\dfrac{\phi(E,r)}{\phi(E,s)}-\dfrac{D(E)+l+1}{2l+1}\left[\dfrac{r}{s}\right]^l & \text{for } r\leq s\\ \dfrac{l-D(E)}{2l+1}\left[\dfrac{r}{s}\right]^{-l-1} & \text{for } r\geq s\end{cases} \tag{2.11}$$

where, again, we have dropped the subscripts R and l. As with the partial wave, the MTO is continuous and differentiable in all space and it is a solution of the Laplace equation outside its sphere. The logarithmic derivative takes the constant value $-l-1$ and the MTO is a regular function, also at infinity.

The tail of an MTO at site $\vec{R}$ may be expanded around site $\vec{R}'$ as follows:

$$\chi_{RL}(E,\vec{r}_R)=-\sum_{L'}\left[\frac{r_{R'}}{a}\right]^{l'}\frac{Y_{L'}(\hat{r}_{R'})}{2(2l'+1)}S_{R'L',RL}\chi_{RL}(E,a)\ , \tag{2.12}$$

where a is an arbitrary scale of the structure, e.g., the lattice constant. The expansion coefficients S are the so-called canonical structure constants which are independent of the lattice constant, the potential, the sphere radii, and the energy. In the representation of the real cubic harmonics they form a real symmetric matrix which is given in Table II of Ref. 20. Expressed as two-center integrals they are simply

$$S_{ss\sigma}=-2(a/d),\quad S_{sp\sigma}=2\sqrt{3}(a/d)^2\ ,$$
$$S_{pp}(\sigma,\pi)=6(a/d)^3(2,-1)\ ,$$
$$S_{sd\sigma}=-2\sqrt{5}(a/d)^3\ ,$$
$$S_{pd}(\sigma,\pi)=6\sqrt{5}(a/d)^4(-\sqrt{3},1)\ ,$$
$$S_{dd}(\sigma,\pi,\delta)=10(a/d)^5(-6,4,-1)\ .$$

Here $d=|\vec{R}-\vec{R}'|$ is the interatomic distance. The lattice constant a has been included in the definition of the structure constants [and of the potential functions in (2.15) below] in order to make them independent of the scale of the structure. In (2.12) the value $\chi(E,a)$ of the radial function at $r=a$ is supposed to be given by that part of (2.11) which is valid for $a\geq s$, regardless of the actual value of a.

A convenient notation may be obtained if we regard the MTO,

$$\chi_{RL}(E,\vec{r}_R)\equiv|\chi(E)\rangle^{\infty}_{RL}\ , \tag{2.13a}$$

the truncated partial wave,

$$\phi_{RL}(E,\vec{r}_R)\Theta(r_R/s_R)\equiv|\phi(E)\rangle_{RL}\ , \tag{2.13b}$$

and the functions,

$$\left[\frac{r_R}{a}\right]^{l}\frac{Y_L(\hat{r}_R)}{2(2l+1)}\Theta(r_R/s_R)=|J\rangle_{RL}\ , \tag{2.13c}$$

as the RL components of the vectors $|\chi(E)\rangle^{\infty}$, $|\phi(E)\rangle$, and $|J\rangle$. The notation $|\ \rangle^{\infty}$ is meant to indicate that the functions (2.13a), in contrast to the functions (2.13b) and (2.13c), extend over all space. With this vector notation the site and angular momentum expansions (2.11) and (2.12) of the MTO may be expressed as

$$|\phi(E)\rangle+|J\rangle[P(E)-S]\chi(E)=|\chi(E)\rangle^{\infty}\ . \tag{2.14}$$

Here S is the structure matrix and $\chi(E)$ and $P(E)$ are diagonal matrices with the components

$$[\chi(E)]_{RL,R'L'}\equiv\chi_{Rl}(E,a)\delta_{RR'}\delta_{LL'}$$

and

$$[P(E)]_{RL,R'L'}\equiv P_{Rl}(E)\delta_{RR'}\delta_{LL'}$$
$$\equiv 2(2l+1)\frac{D_{RL}(E)+l+1}{D_{Rl}(E)-1}\times\left[\frac{a}{s_R}\right]^{2l+1}\delta_{RR'}\delta_{LL'}\ . \tag{2.15}$$

The function $P(E)$ is called the potential function and it is an always increasing tangentlike function of energy. We shall now see that its derivative with respect to energy (the overdot signifying $\partial/\partial E$) is related to $\chi(E,a)$. The energy derivative of the logarithmic derivative function is related to the value of the radial wave function at the sphere through

$$\dot{D}(E)=-\{s[\phi(E,s)]^2\}^{-1}\ , \tag{2.16}$$

as shown, for instance, in Ref. 5. We realize that

$$[\dot{P}(E)]^{-1/2}\equiv\left[\frac{dP}{dE}\right]^{-1/2}$$
$$=\frac{l-D(E)}{2l+1}\left[\frac{s}{a}\right]^{l+1/2}\left[\frac{s}{2}\right]^{1/2}\phi(E,s)$$
$$=(a/2)^{1/2}\chi(E,a)\ , \tag{2.17}$$

where we have used (2.15) and (2.11) and have defined the sign of $\dot{P}^{-1/2}$.

We may now place a linear combination of MTO's at each site of the structure and ask whether we can determine the coefficients such that the linear combination of MTO's

$$\psi(E,\vec{r})=\sum_{R,L}\chi_{RL}(E,\vec{r}_R)B_{RL} \tag{2.18}$$

is a solution of Schrödinger's equation at energy E. The condition is, of course, that the one-center ex-

pansions (2.10) are valid, and this means that inside any sphere the sum of the MTO tails coming from all other sites must cancel the r^l terms [see Eq. (2.11)] from the MTO's located at that site. From (2.14) we thus realize that the matching condition may be expressed analytically as

$$\sum_{R,L}[P_{Rl}(E)\delta_{R'R}\delta_{L'L}-S_{R'L',RL}][\dot{P}_{Rl}(E)]^{-1/2}B_{RL}=0 \tag{2.19}$$

for all R' and L'. These linear homogeneous equations have a nontrivial solution only if the determinant of $\underline{P}(E)-\underline{S}$ vanishes and this condition yields the one-electron energies E_j. The corresponding wave functions are given by the partial-wave one-center expansions (2.10) or, equivalently, by the MTO multicenter expansions (2.18) using the nontrivial solutions $[\dot{P}_{RL}(E_j)]^{-1/2}B_{RL,j}$ of (2.19). The wave function is normalized to unity in all spheres if B is normalized according to

$$\sum_{R,L}|B_{RL}|^2=1\ . \tag{2.20}$$

Equations (2.19) equal the scattered-wave or KKR equations for a MT potential in the limit where the kinetic energy $E-V_{\mathrm{MTZ}}$ in the interstitial region vanishes and the MT spheres are substituted by space-filling atomic spheres. The potential functions are cotangents of the phase shifts in the appropriate limits. The details are given in Appendix A.

The Green-function matrix for the system of equation (2.19) is defined by

$$\sum_{R,L}\{[P_{Rl}(E)-i0^+]\delta_{R'R}\delta_{L'L}-S_{R'L',RL}\}g_{RL,R''L''}(E)=\delta_{R'R''}\delta_{L'L''}\ . \tag{2.21}$$

In terms hereof the imaginary part of the Green function for the Schrödinger equation is

$$\mathrm{Im}G(\vec{r}',\vec{r};E)=\pi\sum_j\psi_j(E,\vec{r}')\psi_j(E,\vec{r})\delta(E-E_j)=|\phi(E)\rangle[\dot{P}(E)]^{1/2}\mathrm{Im}g(E)[\dot{P}(E)]^{1/2}\langle\phi(E)| \tag{2.22a}$$

$$=|\chi(E)\rangle\infty[\dot{P}(E)]^{1/2}\mathrm{Im}g(E)[\dot{P}(E)]^{1/2}\infty\langle\chi(E)|\ , \tag{2.22b}$$

as may be realized from (2.10), (2.14), and (2.18)–(2.20). The entire Green function is derived in Appendix A. The one-center expansion (2.22a) for the Green function converges slowly in L when $\vec{r}$ lies far from the center of any sphere. The MTO multicenter expansion (2.22b), however, converges fast (provided that κ^2 does not differ more than a rydberg or so from the kinetic energy in the outer region of the spheres), and (2.22b) is particularly useful in connection with the Fourier representation of the MTO's given in Ref. 5.

In this paper we shall assume that the spheres are located on a lattice, i.e., that

$$\vec{R}=\vec{T}+\vec{U}\ , \tag{2.23}$$

where $\vec{T}$ are the lattice translations and $\vec{U}$ the sites in the primitive cell. The structure constants are therefore expressed in the Bloch representation,

$$S_{U'L',UL}(\vec{k})=\sum_T\exp(i\vec{k}\cdot\vec{T})S_{U'L',(U+T)L}\ , \tag{2.24}$$

and computed with the Ewald technique.

For the unperturbed crystal the MTO's and the potential functions only depend on $\vec{U}$ and not on $\vec{T}$. The secular equations thus factorize in the Bloch representation, where they equal (2.19) with R substituted by U and S substituted by $S(\vec{k})$. The size of the matrix is now $(l_{\max}+1)^2\approx 9$ times the number of sites in the primitive cell. With B normalized according to $\sum_{U,L}|B_{UL}(k)|^2=1$, the wave function is normalized to unity in the primitive cell. The unperturbed Green-function matrix

$$g^0_{U'L',(U+T)L}(E)=(V_{\mathrm{BZ}})^{-1}\int_{\mathrm{BZ}}d^3k\exp(-i\vec{k}\cdot\vec{T})\{[P^0(E)-i0^+]-S(\vec{k})\}^{-1}_{U'L',UL}\ , \tag{2.25}$$

where V_{BZ} is the Brillouin-zone volume, is tedious to compute by direct means because it requires finding the eigenvalues and eigenfunctions of $\underline{P}^0(E)-\underline{S}(\vec{k})$ as a function of E and $\vec{k}$. In the following we therefore devise a different technique.

B. Hamiltonian matrix and its Green function

The logarithmic derivative function (2.9) for a given partial wave is a cotangentlike function with a branch for each value of the principal quantum

number. The potential function (2.15) is uniquely related to the logarithmic derivative function and has a similar behavior. We are now interested in obtaining the solutions of Schrödinger's equation for the *entire* system in an energy range corresponding to only a *fraction of a branch* and centered at some energy, E_ν. For this purpose we need to parametrize the potential functions $P_{Rl}(E)$ in the form (2.2) and to identify the potential parameters V_{Rl}, Γ_{Rl}, and Q_{Rl}. In addition, we shall need a form more accurate than (2.2) and therefore use the following "linear" approach.[5]

We first parametrize the function $E(P)$, which is inverse to $P(E)$, by setting up a radial trial function $\Phi(D,r)$ with the prescribed logarithmic derivative D or, equivalently, P at the sphere and estimating its energy from the variational principle. The trial function we take as the appropriate linear combination

$$\Phi(D,r)=\phi(E_\nu,r)+\omega(D)\dot{\phi}(E_\nu,r) \tag{2.26}$$

of the normalized (2.7) radial wave function and its first energy derivative function (1.6) at E_ν. The constant ω is given by

$$\omega(D)=-\frac{\phi(E_\nu,s)}{\dot{\phi}(E_\nu,s)}\frac{D-D\{\phi(E_\nu)\}}{D-D\{\dot{\phi}(E_\nu)\}}\ , \tag{2.27}$$

in terms of the amplitudes and radial logarithmic derivatives of ϕ and $\dot{\phi}$ at the sphere. From the radial Schrödinger equation we now obtain

$$(-\nabla^2+v-E_\nu)\,|\,\phi(E_\nu)\rangle=0$$

and

$$(-\nabla^2+v-E_\nu)\,|\,\dot{\phi}(E_\nu)\rangle=|\,\phi(E_\nu)\rangle\ ,$$

and from the choice (2.7) for the normalization of ϕ we have

$$\langle[\phi(E_\nu)]^2\rangle=1$$

and

$$\langle\phi(E_\nu)\,|\,\dot{\phi}(E_\nu)\rangle=0\ .$$

Of the four potential parameters in (2.27), only three are independent because, from Green's second identity,

$$\begin{aligned}1&=\langle[\phi(E_\nu)]^2\rangle=\langle\phi(E_\nu)\,|\,(-\nabla^2+v-E_\nu)\,|\,\dot{\phi}(E_\nu)\rangle\\&=[D\{\phi(E_\nu)\}-D\{\dot{\phi}(E_\nu)\}]s\phi(E_\nu,s)\dot{\phi}(E_\nu,s)\ .\end{aligned}$$

We may now evaluate the energy function from the variational principle and find

$$\begin{aligned}E(P)&\equiv\langle\Phi(D)\,|\,(-\nabla^2+v)\,|\,\Phi(D)\rangle/\langle[\Phi(D)]^2\rangle\\&=E_\nu+\omega(D)\{1+[\omega(D)]^2\langle[\dot{\phi}(E_\nu)]^2\rangle\}^{-1}\ .\end{aligned} \tag{2.28}$$

The trial function (2.26) has errors of second and higher orders in $E-E_\nu$, and the variational estimate (2.28) therefore has errors of fourth and higher orders. From the form of (2.28) we thus realize that the estimate

$$\tilde{E}(P)\equiv E_\nu+\omega(D) \tag{2.29}$$

is correct to second order. In the following we shall invert (2.29) obtaining $\tilde{P}(E)$ and show that it has the form (2.2). A more accurate parametrization of the potential function *correct to third order* is then

$$P(E)=\tilde{P}(E+(E-E_\nu)^3\langle[\dot{\phi}(E_\nu)]^2\rangle)\ , \tag{2.30}$$

as seen from (2.28).

The inversion of (2.29) requires solving (2.27) with respect to D and inserting the result in (2.15). We find

$$\tilde{P}(E)=\frac{E-C}{E-V}Q\equiv\frac{E-C}{\Delta+(E-C)Q^{-1}}\equiv\frac{\Gamma}{V-E}+Q\ , \tag{2.31}$$

where

$$\begin{aligned}Q&\equiv P\{\dot{\phi}(E_\nu)\}\\&=2(2l+1)\frac{D\{\dot{\phi}(E_\nu)\}+l+1}{D\{\dot{\phi}(E_\nu)\}-l}\left[\frac{a}{s}\right]^{2l+1}\end{aligned} \tag{2.32}$$

and

$$C\equiv E_\nu+\omega(-l-1)$$

and

$$V\equiv E_\nu+\omega(l)\ .$$

Moreover,

$$\Delta\equiv(C-V)Q^{-1}$$

and

$$\Gamma\equiv(C-V)Q\ .$$

We have thus proved (2.2) and expressed its three potential parameters in terms of the $\phi,\dot{\phi}$ parameters. The relation of Q, Δ, and Γ to the parameters γ, $\Phi(-l-1,s)$, and $\Phi(l,s)$ used in Refs. 5–9 and 20 is seen to be

$$\begin{aligned}Q&=\frac{1}{\gamma}\left[\frac{a}{s}\right]^{2l+1}\\&=2(2l+1)\frac{\Phi(l,s)}{\Phi(-l-1,s)}\left[\frac{a}{s}\right]^{2l+1}\ ,\\\Delta^{1/2}&=\Phi(-l-1,s)\left[\frac{a}{2}\right]^{1/2}\left[\frac{a}{s}\right]^{-l-1}\ ,\end{aligned} \tag{2.33}$$

and

$$\Gamma^{1/2}=2(2l+1)\Phi(l,s)\left[\frac{a}{2}\right]^{1/2}\left[\frac{a}{s}\right]^{l}.$$

In the two last equations we have defined the signs of $\Delta^{1/2}$ and $\Gamma^{1/2}$. In addition to (2.2) or (2.31) we shall be using the fact that

$$[\dot{\underline{\tilde{P}}}(E)]^{-1/2}=(E\underline{\mathbb{1}}-\underline{V})\underline{\Gamma}^{-1/2}. \tag{2.34}$$

Having parametrized the potential functions we are now in the position to transform the secular equations (2.19) with $P(E)$ substituted by $\tilde{P}(E)$ into eigenvalue equations. We simply multiply (2.19) on the left by the matrix $\underline{\Gamma}^{1/2}(\underline{Q}-\underline{S})^{-1}$ and thereby obtain

$$\begin{aligned}0&=\underline{\Gamma}^{1/2}(\underline{Q}-\underline{S})^{-1}[\underline{\tilde{P}}(E)-\underline{S}][\dot{\underline{\tilde{P}}}(E)]^{-1/2}\underline{B}\\&=\underline{\Gamma}^{1/2}(\underline{Q}-\underline{S})^{-1}[\underline{Q}-\underline{S}+\underline{\Gamma}(\underline{V}-\underline{E})^{-1}](E\underline{\mathbb{1}}-\underline{V})\underline{\Gamma}^{-1/2}\underline{B}=(E\underline{\mathbb{1}}-\underline{H})\underline{B}\end{aligned} \tag{2.35}$$

with

$$\underline{H}\equiv\underline{V}+\underline{\Gamma}^{1/2}(\underline{Q}-\underline{S})^{-1}\underline{\Gamma}^{1/2}, \tag{2.3'}$$

which is (2.3). An equivalent expression for the Hamiltonian is

$$\underline{H}\equiv\underline{C}+\underline{\Delta}^{1/2}\underline{S}(\underline{\mathbb{1}}-\underline{Q}^{-1}\underline{S})^{-1}\underline{\Delta}^{1/2}. \tag{2.36}$$

In the matrix equations above, $\underline{\tilde{P}}(E)$, $\underline{V}$, $\underline{Q}$, $\underline{\Gamma}$, $E\underline{\mathbb{1}}$, etc., are regarded as matrices diagonal in R and L, exactly as in (2.14) and (2.15).

The secular equation (2.19) with $\underline{P}$ substituted by $\underline{\tilde{P}}$ is thus equivalent with the eigenvalue equation (2.35) for the Hermitian Hamiltonian (2.3) or (2.36). The eigenvalues of H equal the one-electron energies to second order in $E-E_\nu$. The Hamiltonian H effectively has the two-center form with hopping integrals factorized into potential parameters Δ, which specify the bandwidth and the strength of the hybridization, and screened structure constants $\underline{S}(\underline{\mathbb{1}}-\underline{Q}^{-1}\underline{S})^{-1}$. We use the name *screened* structure constants because the matrix elements decrease exponentially with interatomic distance while those of S decrease as $d^{-l-l'-1}$.

It may be shown[7] that H is the Hamiltonian in the representation of the following energy-independent orbitals:

$$|\phi(E_\nu)\rangle+|\dot{\phi}(E_\nu)\rangle(\underline{H}-E_\nu\underline{Q})\equiv|\theta\rangle^{\infty}. \tag{2.37}$$

Here we have used the same notation as in (2.14). The θ orbitals (2.37) are orthogonal to first order in $\underline{H}-E_\nu\underline{\mathbb{1}}$, so that their overlap matrix $\underline{Q}$ equals the unit matrix to first order in $\underline{H}-E_\nu\underline{\mathbb{1}}$.

The Green function for the Hamiltonian is defined by the matrix equation

$$[(E-i0^+)\underline{\mathbb{1}}-\underline{H}]\underline{\tilde{G}}(E)=\underline{\mathbb{1}}, \tag{2.38}$$

and the relation to the Green function (2.21) for the secular equation is easily found from (2.35) to be

$$\begin{aligned}\tilde{g}(E)\equiv[\tilde{P}(E)-S]^{-1}&=[\dot{\tilde{P}}(E)]^{-1/2}\tilde{G}(E)\Gamma^{1/2}(Q-S)^{-1}=[\dot{\tilde{P}}(E)]^{-1/2}\tilde{G}(E)(H-V)\Gamma^{-1/2}\\&=[\dot{\tilde{P}}(E)]^{-1/2}[-1+\tilde{G}(E)(E-V)]\Gamma^{-1/2}=-\frac{E-V}{\Gamma}+\frac{E-V}{\Gamma^{1/2}}\tilde{G}(E)\frac{E-V}{\Gamma^{1/2}}.\end{aligned} \tag{2.39}$$

We therefore have

$$\mathrm{Im}\tilde{G}(E)=[\dot{\tilde{P}}(E)]^{1/2}\mathrm{Im}\tilde{g}(E)[\dot{\tilde{P}}(E)]^{1/2}, \tag{2.40}$$

which is in accordance with the more general relation (2.22).

The transformation (2.39) is simply a scaling because $(E\underline{\mathbb{1}}-\underline{V})\underline{\Gamma}^{-1/2}$ is diagonal in R and L. The relation to the Green function for the Schrödinger equation is given in Appendix A where the exact definition of $G(E)$, which reduces to $\tilde{G}(E)$ when $\underline{P}$ is substituted by $\underline{\tilde{P}}$, may be found in (A27), (A32), and (A34).

C. Application to the impurity problem

For the unperturbed crystal we first diagonalize the Hamiltonian

$$H^0_{UL,U'L'}(\vec{k})=V^0_{UI}\delta_{UU'}\delta_{LL'}+(\Gamma^0_{UI})^{1/2}\{[Q^0-S(\vec{k})]^{-1}\}_{UL,U'L'}(\Gamma^0_{U'I'})^{1/2}, \tag{2.41}$$

and thus find the energy bands $E_j^0(\vec{k})$ and normalized eigenvectors $B_{UL,j}^0(\vec{k})$ at a large number of $\vec{k}$ points in the Brillouin zone. The size, M^0, of H^0 is $(l_{\max}+1)^2$, typically equal to 9 times the number of sites in the primitive cell. With the tetrahedron method[21] we then compute the projected densities of states,

$$N_{U'L',(U+T)L}^0(E)=(V_{\mathrm{BZ}})^{-1}\sum_j \int \exp(i\vec{k}\cdot\vec{T})B_{U'L',j}^{0*}(\vec{k})B_{UL,j}^0(\vec{k})\delta(E-E_j(\vec{k}))d^3k \ , \tag{2.42}$$

involving the sites at which the potential is going to be perturbed. The unperturbed Green-function matrix is now given by

$$\mathrm{Im}\tilde{G}^0(E)=\pi N^0(E) \tag{2.43}$$

and

$$\mathrm{Re}\tilde{G}^0(E)=\mathscr{P}\int \frac{N^0(E')}{E-E'}dE' \ , \tag{2.44}$$

and, finally, the real and imaginary parts of $\tilde{g}^0(E)$ may be found using (2.39).

We emphasize that it is the Hamiltonian formulation (2.35), which is correct to order $(E-E_v)^2$, that makes it a rather simple matter to calculate the unperturbed Green function. Moreover, the Hilbert transformation (2.44) is straightforward because the M^0 energy bands of H^0 have finite extent. This simplification does, for instance, not occur in the KKR Green-function method.

In order to solve the Dyson equation (2.1) we need the matrix elements of the unperturbed Green function for R and R' running over all sites in the perturbed region. Because of the symmetries in the space group of the unperturbed crystal, many of the quantities $N_{R'L',RL}^0$ in (2.42) are related by symmetry and only a few need to be calculated. For the perturbed crystal the symmetry is, in general, lower and we are left with a point group of rotations $\hat{\mathscr{R}}$. It is important to use this symmetry to keep the matrices at a manageable size. Following Slater[22] we now transform from the previously used site and real spherical harmonic representation (2.6) to the symmetry representation given by the following functions:

$$f_{\kappa\mu,RL}^{\alpha}(\vec{r})=\sum_{\mathscr{R}}\Gamma_{\kappa\mu}^{\alpha}(\mathscr{R})\hat{\mathscr{R}}\phi_{RL}(\vec{r}_R)\Theta(r_R/s_R) \ . \tag{2.45}$$

Here $\Gamma_{\kappa\mu}^{\alpha}(\mathscr{R})$ are the matrices of the αth irreducible representation of the point group. Although R runs over one site per shell only, the functions f are linearly dependent in general. Thus we only keep a smaller number of linearly independent functions and, from them, form a orthonormal basis set. Finally, the projected densities of states (2.42), and with these the unperturbed Green function (2.43) and (2.44), are transformed into the orthonormal symmetry representation.

To solve the Dyson equation (2.1) we further need $\Delta P(E)\equiv P(E)-\tilde{P}^0(E)$. For the latter we use (2.2) and for the former we can obtain any desired accuracy. We have used the third-order expansion (2.30). In the following we shall for simplicity of notation drop the tilde on P^0 and g^0.

We are now in the position to solve the Dyson equation and need only consider the small block (2.1b) which, due to the point symmetry, is even smaller than 9 times the number of perturbed sites. In the following we shall use matrix notation and let g_M denote the small block with matrix elements g_{ij} where i and j now refer to the orthonormal symmetry representation.

From (2.1b) we see that there is a bound state at an energy $E=E_b$ if

$$\det[\underline{1}+g_M^0(E_b)\Delta\underline{P}(E_b)]=0 \tag{2.46}$$

and $\mathrm{Im}g_M^0(E_b)=0$. We thus search for the zeros of (2.46) below the bottom of the band and in the band gaps. In order to obtain the bound-state wave function, or rather $\mathrm{Im}g_M(E_b)$, we diagonalize the matrix

$$\{[\underline{g}_M^0(E)]^{-1}+\Delta\underline{P}(E)\}\equiv[\underline{g}_M(E)]^{-1} \tag{2.47}$$

for a few energies in the neighborhood of E_b, obtaining the eigenvalues $p_j(E)$ and eigenvectors $X_j(E)$. We shall only be interested in that value (those values, in case of degeneracy) of j for which $P_j(E_b)=0$. It may be noted in passing that if M had included the entire system, then $[g_M(E)]^{-1}$ would simply have been $P(E)-S$. We may now invert $[g_M(E)]^{-1}$, obtaining

$$g_M(E)=\sum_j X_j(E)[p_j(E)-i0^+]^{-1}X_j^+(E) \ , \tag{2.48}$$

and consequently the result

$$\mathrm{Im}g_M(E_b)=\pi\sum_j X_j(E_b)[\dot{p}_j(E_b)]^{-1}\times\delta(E_j-E_b)X_j^+(E_b) \ . \tag{2.49}$$

The energy derivative of the nearly vanishing eigenvalue is found numerically. For an energy in the

continuum we treat (2.1b) as a set of linear inhomogeneous equations and solve for $g_M(E)$.

The induced total density of states, integrated over the *entire* system, is

$$N(E)-N^0(E)=\pi^{-1}\mathrm{Im}[\mathrm{Tr}G(E)-\mathrm{Tr}G^0(E)] , \tag{2.50}$$

and since

$$\mathrm{Tr}\underline{G}(E)=-\frac{d}{dE}\ln\det\underline{G}(E) ,$$

as is easily proved in the eigenrepresentation of G, one finds[13]

$$N(E)-N^0(E)=\pi^{-1}\dot{\eta}(E) , \tag{2.51}$$

where the generalized phase shift is defined as

$$\eta(E)\equiv\arg\det\{\underline{G}^0(E)[\underline{G}(E)]^{-1}\} , \tag{2.52}$$

where arg = Im ln. This expression also holds when the G's are substituted by the g's because we may use (2.40) plus the fact that $[P(E)]^{-1}$ and $\dot{P}^0(E)$ are real. According to (2.1a), we know that $\underline{g}^0\underline{g}^{-1}=\underline{\mathbb{1}}+\underline{g}^0\Delta\underline{P}$ and, if we now expand $\det[\underline{\mathbb{1}}+\underline{g}^0\Delta\underline{P}]$ after the last columns, we realize that it equals $\det[\mathbb{1}+\underline{g}^0_M\Delta\underline{P}]$. As a result,

$$\eta(E)=\arg\det[\underline{\mathbb{1}}+\underline{g}^0_M(E)\Delta\underline{P}(E)] . \tag{2.53}$$

Owing to symmetry, $\mathbb{1}+\underline{g}^0_M\Delta\underline{P}$ is usually block diagonal and the determinant factorizes. The generalized phase shift (2.53) is thereby expressed as the sum of the phase shifts $\eta_\alpha(E)$ for the different irreducible symmetry representations.

The charge density in the perturbed region may be obtained from $\mathrm{Im}g_M(E)$ by first transforming it from the symmetry representation and back into the site and angular momentum representation. Then we use (2.22) with $\vec{r}=\vec{r}'$ and obtain for the spherically symmetrized valence charge density,

$$n_{v;R}(r)=(4\pi)^{-1}\sum_l\int^{E_F}[\phi_{Rl}(E,r)]^2N_{Rl}(E)dE , \tag{2.54}$$

where

$$N_{Rl}(E)\equiv\pi^{-1}\dot{P}_{Rl}(E)\sum_m\mathrm{Im}g_{Rlm,Rlm}(E) . \tag{2.55}$$

For the radial wave functions we use the Taylor series (1.6) to second order in $E-E_\nu$. The charge density (2.54) is thus given in terms of ϕ, $\dot{\phi}$, and $\ddot{\phi}$ and the zeroth- through fourth-energy moments of $N_{Rl}(E)$.

The one-electron potential in the sphere at site R is

$$v_R(r)=\mu_{\mathrm{xc}}(n_{vc;R}(r))+2\int_R\frac{n_{vc;R}(r')}{|\vec{r}-\vec{r}'|}d^3r' -\frac{2Z_R}{r}+\sum_{R'}{}'\frac{2q_{R'}}{|\vec{R}-\vec{R}'|} \tag{2.56}$$

in the ASA. The first term is the exchange-correlation potential in the local approximation[19] and $n_{vc}\equiv n_v+n_c$ is the density of the valence and core electrons. The former is obtained from (2.54) and the latter is taken from a free-atom calculation, that is, we use the frozen-core approximation. The second term is the electrostatic potential from the valence- and core-electron density. The integral is in the sphere and, in the ASA where only the spherical average of the density is used, the integral reduces to the sum of two radial integrals. The third term is the electrostatic potential from the nucleus and the fourth term is the electrostatic Madelung potential from the net charges q in all other spheres. Here

$$q_R\equiv-Z_R+\int_R n_{vc;R}d^3r=-z_R+\int_R n_{v;R}d^3r , \tag{2.57}$$

and Z is the atomic number and z the valency.

The Madelung potential at site R in the unperturbed crystal $v^0_{M;R}$ is computed with the Ewald procedure and may, in fact, be obtained from $l=l'=0$ matrix elements of the structure constants. For the crystal with the impurity

$$v_{M;R}=v^0_{M;R}+\sum_{R'}{}'\frac{2\Delta q_{R'}}{|\vec{R}-\vec{R}'|} , \tag{2.58}$$

where R' runs over the perturbed sites *plus* their nearest neighbors. The reason for this is that we do not, in general, obtain complete charge neutrality in the perturbed region because there is also a small change in the charge density outside this region. This charge we assume to be located in the spheres closest to the perturbed region. This is important for the convergence of the self-consistent calculations, since a small change in the potential can lead to a substantial flow of charge out of the perturbed region. The complete neglect of this charge would lead to a large change in the potential and poor convergence.

Equation (2.56) only holds for the fully self-consistent potential. In practice, the charge obtained from the nth iteration defines through (2.56) a potential which is subsequently mixed with the potential of the nth iteration to form the potential for the $(n+1)$st iteration.

D. Total energy

In the Born-Oppenheimer, the local-density, and the AS approximations, the total energy may be expressed as

$$\mathscr{E}=\sum_R\sum_{R'}{}'\frac{q_R q_{R'}}{|\vec{\mathrm{R}}-\vec{\mathrm{R}}'|}+T_{vc}+\sum_R\int_R n_{vc;R}(r)\left[\int_R\frac{n_{vc;R}(r')}{|\vec{\mathrm{r}}-\vec{\mathrm{r}}'|}d^3r'-\frac{2Z_R}{r}+\epsilon_{\mathrm{xc}}(n_{vc;R}(r))\right]d^3r \tag{2.59}$$

$$=\sum_R\tfrac{1}{2}v_{M;R}q_R+\int^{E_F}EN(E)dE+\sum_R\int_R n_{v;R}(r)[-v_R(r)+\tfrac{1}{2}v_{v;R}(r)+v_{cn;R}(r)]d^3r$$

$$+\sum_R\int_R[n_{vc;R}(r)\epsilon_{\mathrm{xc}}(n_{vc;R}(r))-n_{c;R}(r)\epsilon_{\mathrm{xc}}(n_{c;R}(r))]d^3r$$

$$+\sum_R\left[T_{c;R}+\int_R n_{c;R}(r)\left[\tfrac{1}{2}v_{c;R}(r)-\frac{2Z_R}{r}+\epsilon_{\mathrm{xc}}(n_{c;R}(r))\right]d^3r\right]. \tag{2.60}$$

In (2.59), the first term is the electrostatic interaction between the spheres, the second term is the sum of the single-particle kinetic energies of the valence (v) and core (c) electrons (T_{vc}), and the third term is the sum of the intrasphere interactions between the electrons and between the electrons and the nucleus (n). The integral is in the sphere at R.

In (2.60) we have expressed the electrostatic interaction between the spheres in terms of the Madelung (M) potential $v_{M;R}$ defined in (2.58). The kinetic energy of the valence electrons has been written as the sum of the single-particle energies of the valence electrons, expressed in terms of their density of states $N(E)$ given by (2.42) and (2.51), minus the potential energy of the valence electrons as specified by the one-electron potential v_R in (2.4). The electrostatic (Hartree) potential from the valence electrons in the sphere is $v_{v;R}$ and the electrostatic potential from the core electrons and the nucleus in the sphere is $v_{cn;R}$. The last term in (2.60) contains core quantities only, and, in the frozen-core approximation, this term is the same as for free atoms. In the following we shall drop this core term and, when calculating heats of formation, assume that the same has been done in the calculations for the free atoms. The remaining last but one term in (2.60) is the rather small difference between the total exchange-correlation energy and the exchange-correlation energy between the core electrons.

In (2.60) we let the single-particle potential v_R be the one used in the last iteration, while all other potentials are obtained from the valence charge density resulting from that iteration. Then the total energy is of second order in the deviation of the density from the converged one. [With this definition v_R need not be fully self-consistent and (2.56) need therefore not be satisfied.] This ensures rapid convergence of the total energy, which then converges faster than the one-electron energies.

We want to calculate the change $\Delta\mathscr{E}\equiv\mathscr{E}-\mathscr{E}^0$ of the total energy when an impurity is introduced. The difference between the perturbed and the unperturbed expression (2.60), minus the core term $\mathscr{E}_c$, yields

$$\Delta\mathscr{E}-\Delta\mathscr{E}_c=\int^{E_F}E\Delta N(E)dE+\sum_R v^0_{M;R}\Delta q_R+\sum_R\sum_{R'}{}'\frac{\Delta q_R\Delta q_{R'}}{|\vec{\mathrm{R}}-\vec{\mathrm{R}}'|}$$

$$+\sum_R\int_R n^0_{v;R}(r)[-\Delta v_R(r)+\Delta v_{cn;R}(r)]d^3r$$

$$+\sum_R\int_R[-v_R(r)+v^0_{v;R}(r)+\tfrac{1}{2}\Delta v_{v;R}(r)+v_{cn;R}(r)]\Delta n_{v;R}(r)d^3r$$

$$+\sum_R\Delta\int_R[n_{vc;R}(r)\epsilon_{\mathrm{xc}}(n_{vc;R}(r))-n_{c;R}(r)\epsilon_{\mathrm{xc}}(n_{c;R}(r))]d^3r\,, \tag{2.61}$$

where v^0_M, n^0_v, and v^0_v refer to the unperturbed crystal while v and v_{cn} refer to the crystal with the impurity.

In (2.61) the R sums are seen to run only over those spheres where the *density* is perturbed. In the calcula-

tions, we shall further restrict the sums to those sites where the *potential* is perturbed. This is, in fact, correct to first order in the induced density because, for a site where $v_R = v_R^0$ and $v_{cn;R} = v_{cn;R}^0$, we have $\Delta n_R = \Delta n_{v;R}$ and the corresponding terms in (2.61) are

$$\int_R [v_{M;R}^0 - v_R^0(r) + v_{v;R}^0 + v_{cn;R}^0(r)]\Delta n_{v;R}(r)d^3r + \Delta \int_R n_{vc;R}(r)\epsilon_{xc}(n_{vc;R}(r))d^3r \tag{2.62}$$

to first order in Δn_R. To this order the last term, however, equals

$$\int_R \mu_{xc}(n_{vc;R}(r))\Delta n_{v;R}(r)d^3r \ , \tag{2.63}$$

and using now (2.56), which holds to first order, we realize that (2.62) vanishes.

The sum of the one-electron energies may be expressed in terms of the generalized phase shifts (2.52) by performing a partial integration and using (2.51). We obtain

$$\int^{E_F} E\Delta N(E)dE = E_F \Delta z - \frac{1}{\pi}\int^{E_F} \eta(E)dE \ , \tag{2.64}$$

where Δz is the valency change. This expression is relatively insensitive to violations of Friedel's sum rule since we have used explicitly the fact that the number of induced states should equal the net change of the valencies.

The major approximation in our total-energy expression (2.60) and (2.61) is the ASA, as used for calculating the interaction energies. We note, however, that it should be possible to calculate these without spherically symmetrizing the charge densities. The ASA could be kept for calculating the kinetic energy and, hence, during the self-consistent one-electron calculation. This would lead to results for the total energy which are correct to first order in the deviations from the ASA and therefore better than the results presented here.

III. APPLICATIONS

In this section we study the accuracy of our method and isolate the sources of the errors. For this purpose it is useful to choose model problems which are simple enough to allow an exact solution but also can be solved by our method in such a way that its approximations are tested.

A. Hulthén potential

We first test our solution of Schrödinger's equation for a given potential. Specifically, we consider an impurity in jellium and assume that the (screened) impurity potential is of the Hulthén form

$$V(r) = -U/(e^{r/\lambda} - 1) \ , \tag{3.1}$$

where U and λ are constants to be determined below. For small r the Hulthén potential behaves as a Coulomb potential

$$\lim_{r\to 0} V(r) = -\frac{\lambda U}{r} \ , \tag{3.2}$$

and for large values it decays exponentially,

$$\lim_{r\to\infty} V(r) = -Ue^{-r/\lambda} \ . \tag{3.3}$$

This potential is a fairly good approximation to the Thomas-Fermi potential and it is possible to determine analytically both the s phase shift and, if the potential is strong enough to bind a state, the energy of the bound s state.[23]

We consider an impurity with a valency one unit larger than the valency of the host, and choose $U\lambda = 2$ to obtain the proper behavior for small distances. We use $\lambda = \sqrt{r_s}/1.5632$ which gives essentially Thomas-Fermi screening, and take $r_s = 2.67$ which corresponds to the density of the s electrons in Cu metal. This leads to $\lambda = 1.05$.

In order to test our method we assume that the unperturbed jellium has a lattice structure. At each lattice site we locate a sphere with the Wigner-Seitz radius s so that space is filled with slightly overlapping spheres. The impurity is located at one of the lattice sites and the perturbing potential extends into the other atomic spheres. This potential is spherically symmetric in the central sphere but nonspherical in all other spheres. In the ASA we replace the true potential in each of these noncentral spheres by its spherical average relative to the center of that sphere. Our LMTO-ASA method now has essentially four sources of error: In the calculation of the unperturbed Green function we (i) use an approximation $\tilde{P}^0(E)$ to the correct unperturbed potential function $P^0(E)$ and (ii) we assume that the atomic spheres fill all of space, neglecting the fact that they overlap. In the solution of the Dyson equation, we (iii) use the same geometry violation, and (iv) neglect the nonspherical potential components. When solving the Dyson equation we can use the exact perturbed potential functions and no essential additional errors are introduced. The assumption of a spherical potential in the calculation of the unperturbed Green function is exact for a homogeneous jellium and it should also be good for closely packed metals. Even for semiconductors it gives satisfactory accuracy provided that empty as well as atomic spheres

TABLE I. The bound-state energy for the Hulthén potential with parameters appropriate for a divalent impurity in copper ($\Delta z=1$, $s=2.67$, $\lambda=1.05$). The exact unperturbed lattice Green function given in Appendix B has been used. "1 shell" means that the perturbing Hulthén potential is taken into account on the central site only. "2 shells" means that the potential inside the neighboring spheres is included also. The number of partial waves considered is indicated by the notations *s*, *sp*, *spd*, and *spdf*. The nonspherical correction estimated with first-order perturbation theory has been added to the result for two shells with *s*, *p*, and *d*, and *f* waves.

ASA, exact g^0		E_b (mRy)
1 shell		−258
2 shells	*s*	−261
	sp	−262
	spd	−263
	spdf	−263
	+ nonspherical	−276
Exact		−272

are used.[18] In the perfect crystal many of the nonspherical components of the potential are zero due to symmetry. For the impurity system, however, there are fewer symmetry restrictions on the potential and (iv) deserves careful consideration.

We now study these errors using the Hulthén potential together with the lattice structure (fcc) and the AS radius ($s=2.67$) of copper. With the parameters defined above, the Hulthén potential has a bound *s* state but no bound states with higher *l* quantum numbers. In Table I we show some results for the bound state. In this calculation we have used the exact unperturbed lattice Green function of Appendix B and the errors are therefore due to approximations (iii) and (iv). The table gives the results obtained for the cases when the impurity potential is assumed to be limited to the atomic sphere surrounding the impurity (1 shell) and to this sphere plus the 12 spheres on the neighboring sites (2 shells). Inclusion of second-nearest neighbors has a negligible effect. To describe the *s*-like bound state we need only *s* partial waves in the central sphere, while higher partial waves contribute in the neighboring spheres. The inclusion of *s*, *p*, and *d* waves leads to good convergence, and adding *f* waves only changes the result by 0.1 mRy. The errors (iii) and (iv) of the ASA thus amount to 9 mRy.

To see the effect of the neglected nonspherical potential components (iv) we use first-order perturbation theory. In this case, when the bound state is far below the bottom of the continuum, perturbation theory gives a good estimate as can be seen from the following test: To estimate the position of the bound state when only the central-cell potential is included, we calculate the expectation value

$$\int_{r>s} d^3r\, V(r)\psi(r)^2$$

of the impurity potential $V(r)$ outside the central cell using the exact wave function $\psi(r)$. We then subtract this integral from the exact bound-state energy and obtain the perturbational estimate −0.257 Ry. This agrees well with the value −0.258 in Table I, and it is an upper estimate as it should be. Thus perturbation theory should be valid also for the weaker nonspherical potential. We calculate

$$\int d^3r[V(r)-V_{\rm AS}(\vec{r})]\psi(r)^2\ ,$$

where $V_{\rm AS}(\vec{r})$ is the AS potential (2.4) used in the calculation. This leads to a correction of 13 mRy and, hence, a result 4 mRy below the exact one.

The geometry violation (iii) therefore tends to lower the bound state by about 4 mRy and the neglect of the nonspherical components tends to raise it by 13 mRy. This adds up to the total ASA error of 9 mRy shown in Table I.

In Table II we show results obtained using the calculated (approximate) unperturbed Green function defined in Secs. II B and II C. Several different values of E_ν were used in the calculation of $\tilde{G}^0$. As perturbation in the Dyson equation we consider both the difference $P(E)-P^0(E)$ and, more appropriately, $P(E)-\tilde{P}^0(E)$. Inside the perturbed region, we correct in the latter case for the use of an approximate potential function $\tilde{P}^0$ when calculating the unperturbed Green function. This was discussed in Sec. II. By comparing the results in Table II for $E_\nu=-0.25$ Ry$\approx E_b$ with the ones in Table I, we see

TABLE II. The bound-state energy for the Hulthén potential using the approximate unperturbed Green function $\tilde{g}^0$ calculated for the E_ν shown. In the column $\Delta P=P-P^0$ we use the exact change of *P*, while under $\Delta P=P-\tilde{P}^0$ we correct inside the perturbed region for the approximation to P^0 used in the calculation of $\tilde{g}^0$. In the second shell *s*, *p*, and *d* partial waves were included.

ASA, approximate $\tilde{g}^0$		E_b (mRy)	
E_ν (mRy)	shells	$\Delta P=P-P^0$	$\Delta P=P-\tilde{P}^0$
−250	1	−260	−260
−250	2	−264	−264
0	1	−263	−259
0	2	−267	−264
250	1	−290	−261
250	2	−293	−264
500	1	−353	−266
500	2	−355	−264
Exact		−272	

that the errors due to the geometry violation (ii) are small and of the order of 1 mRy. The error (i) due to the use of an approximation $\tilde{P}^0$ when calculating the unperturbed Green function is also small provided that we use $\Delta P = P - \tilde{P}^0$. Even for $E - E_\nu = 0.75$ ($E_\nu = 0.5$) the error is just 6 mRy when only the central site is considered. Including also the perturbation on the nearest-neighbor sites means that we correct $\tilde{P}^0$ over a larger region. We see that in this way the error is reduced to below 1 mRy.

It is also instructive to compare the ASA with the MT approximation in which the spheres touch each other without overlap. The MT approximation does not violate the geometry but the perturbing potential is, on the other hand, limited to inside the MT spheres since the impurity cannot shift the MT zero. We have made the comparison between the ASA and MT approximation both for a Cu fcc lattice as above, and for a fictitious Cu bcc lattice with the same atomic volume. The results are shown in Table III.

Since the MT approximation is exact for the unperturbed homogeneous jellium we only use the exact unperturbed lattice Green function together with the MT approximation while, for the ASA calculation, we also consider the approximate unperturbed Green function described in Secs. II B and II C. The ASA approximation is seen to be about a factor of 2 better than the MT approximation. The reason is that in both cases the perturbation can only be taken into account inside the spheres. Thus in the ASA approximation where the spheres fill space, the perturbing potential is fairly well treated although we pay a certain price in terms of a geometry violation. In the MT approximation, on the other hand, the perturbation is neglected in the interstitial region which amounts to nearly one-third of the volume. For a bcc lattice, for instance, we find from perturbation theory that the neglected potential in the interstitial region accounts for about 19 mRy, i.e., 80% of the error, while the neglected nonspherical part of the potential inside the MT spheres only contributes about 5 mRy.

TABLE III. Bound-state energy for the Hulthén potential in a fcc and bcc lattice with the same atomic volume. In the MT calculation we have used the exact unperturbed lattice Green function while, in the ASA, we have tested also the approximate $\tilde{g}^0$ calculated in Sec. II. For the latter, $E_\nu = -0.25$ Ry so that $\tilde{g}^0 \approx g^0$. The perturbation was limited to the first two shells, and s, p, d, and f waves were included.

	E_b (mRy)	
	fcc	bcc
ASA, approximate $\tilde{g}^0$	−264	−262
ASA, exact g^0	−263	−263
MT, exact g^0	−252	−248
Exact	−272	

We now turn to our calculation of the continuous part of the spectrum. We study the generalized phase shifts $\eta(E)$ [Eq. (2.53)] which give the number of induced states below the energy E. In particular, we consider the representations which include the s, p, and d partial waves at the central atom and label the phase shifts accordingly. These are compared with the exact phase shifts for the Hulthén potential. In Fig. 1 we show the results. For the d phase shift our (approximate) calculations give two values corresponding to the E_g and T_{2g} representations, and in the figure we show the average $\eta_d = \frac{2}{5}\eta_{E_g} + \frac{3}{5}\eta_{T_{2g}}$. The ASA calculation is quite accurate for small energies and the errors increase with energy. The results were obtained using $E_\nu = 0.25$ Ry in the calculation of $\tilde{G}^0$. By comparing with the results obtained using $E_\nu = 0$ and 0.5 Ry, which are correct around $E = 0$ and 0.5 Ry, respectively, we conclude that the error (i) due to the use of $\tilde{P}^0(E)$ with $E_\nu = 0.25$ Ry is small over the entire energy range. Comparison between calculations using the exact (Appendix B) and the approximate unperturbed Green function also shows that the geometry violation (ii) is not particularly important. The deviations are mainly due to the neglect of the nonspherical components of the perturbing potential (iv) and to a smaller extent the geometry violation (iii). We have also performed calculations for a bcc lattice with the same AS radius. The deviations tend to be slightly larger for the s and p phase shifts and somewhat smaller for the d phase shift.

In Fig. 1 we also show results obtained with the MT approximation. As for the bound state the ASA is generally more accurate than the MT approximation, where the errors are typically twice as large.

The present application of our method to an impurity in jellium is probably a rather stringent test. For the case of an impurity in a transition metal, for instance, we expect the d waves to be more localized to the central parts of the atomic cells and, in this case, the geometry violation in the ASA should be less serious. The nonspherical components of the perturbing potential also decrease in importance.

B. Self-consistent calculations

In the preceding section we applied our method to the impurity problem for a *given* potential, the Hulthén potential. Now we solve self-consistently the problems of the free hydrogen atom, a proton in

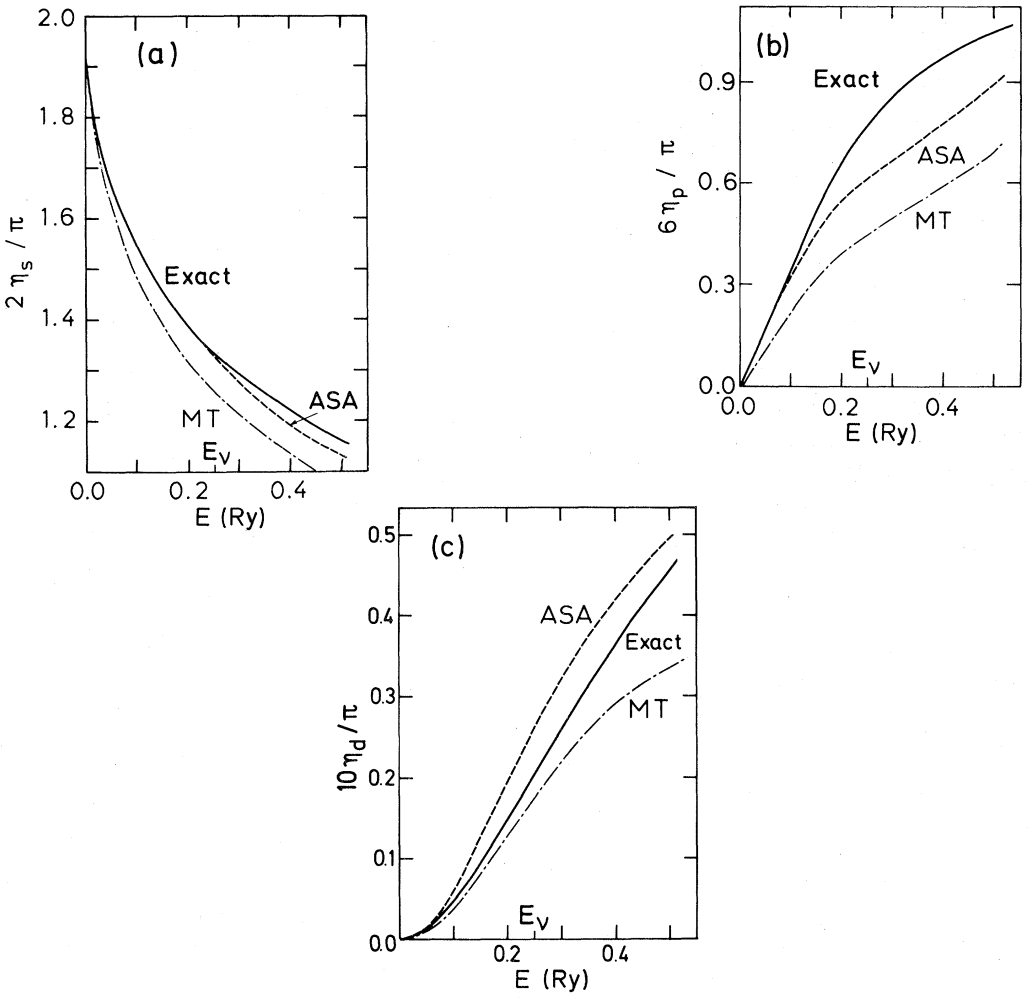

FIG. 1. Generalized phase shift η [Eq. (2.53)] for the Hulthén potential as a function of the energy E. The figure shows the exact result (solid line), the LMTO-ASA result (dashed line), and the MT result (dashed-dotted line).

jellium, and lithium in jellium, using the local-density approximation. For these problems nearly exact solutions are available. This provides further tests of our method, in particular, of our calculation of the self-consistent potential and the total energy.

We first study the accuracy of our total-energy expression and consider a "truncated" hydrogen atom for which the one-electron potential vanishes outside a sphere of radius s^*. We occupy the bound state with one electron and leave the continuum states empty. From this charge density a new potential is calculated and the problem is solved self-consistently. Exchange and correlation effects are included through the local-spin-density (LSD) approximation.[24] We note that if s^* were made infinitely large this approach should lead to the exact LSD result. To illustrate how the result converges with the size of the region which is considered per-

TABLE IV. Local-density calculation for a truncated hydrogen atom, whose potential is localized to a sphere of radius s^*. The results for $s^*=\infty$ have been obtained from an atomic program. The total energy is given by $\mathscr{E}$ and the energy eigenvalue by E_b. To illustrate the rapid convergence of the total energy we also show the kinetic energy inside the sphere, $T_{\text{exact}}=4\pi\int_0^{s^*} r^2\,|\nabla\psi(r)|^2 dr$ calculated for the exact hydrogen wave function.

s^* (a.u.)	$\mathscr{E}$ (Ry)	E_b (Ry)	T_{exact} (Ry)
2.0	−0.8954	−0.4643	0.7619
2.5	−0.9434	−0.5148	0.8753
2.982	−0.9615	−0.5371	0.9380
3.5	−0.9692	−0.5481	0.9704
4.0	−0.9721	−0.5528	0.9862
4.5	−0.9733	−0.5548	0.9938
5.0	−0.9737	−0.5555	0.9972
∞	−0.9740	−0.5560	1.0000

TABLE V. Local-density calculations for a free hydrogen atom using two shells of spheres and the fcc lattice structure of Al. The total energy is $\mathscr{E}$ and the energy eigenvalue E_b. The exact result is obtained from an atomic calculation and the approximate $\tilde{g}^0$ was calculated for $E_\nu=-560$ mRy.

	$\mathscr{E}$ (mRy)	E_b (mRy)
ASA, approximate $\tilde{g}^0$	−970	−558
ASA, exact g^0	−969	−555
MT, exact g^0	−957	−543
Exact	−974	−556

turbed, we show in Table IV results for the total energy $\mathscr{E}$ and the energy eigenvalue E_b as functions of s^*. The results for $s^*=\infty$ are the exact LSD results for the functional used. To illustrate that the total energy converges faster than the individual contributions, we show the kinetic energy calculated from the formula

$$T_{\text{exact}}(s^*)=\int_{r\le s^*} d^3r\,|\nabla\psi(r)|^2$$

using the exact H wave function. For the hydrogen atom, where $\psi(r)\propto\exp(-r)$, this expression is also numerically equal to the number of electrons inside the sphere. For $s^*=4$, for instance, $\mathscr{E}$ is only 0.2% from the exact LSD $s^*=\infty$ value while $T_{\text{exact}}(s^*)$ is still off by 1.4%.

As a test of the LMTO-ASA method, we now consider a free ($s^*=\infty$) hydrogen atom. As in the preceding section we fill space with overlapping atomic spheres. We assume parameters corresponding to Al and use the sphere radius $s=2.982$ and an fcc lattice. As before we use the spherical average of the potential inside each sphere. Table V shows results for a two-shell calculation, which includes the central sphere and the shell of the 12 nearest neighbors. The radius of a sphere with the same volume as the atomic spheres in the central and nearest shells is 7.0 and, for this value of s^*, both $\mathscr{E}$ and E_b are converged to the exact LSD results to within 1 mRy (Table IV). The errors in Table V are therefore not due to the neglect of the third shell. In the calculation of the unperturbed approximation Green function (Sec. II) we have used $E_\nu=-0.56$ Ry. The ASA calculation agrees with the exact one to within 2 and 4 mRy for the energy eigenvalue and the total energy, respectively. If we use the proper perturbation $\Delta P=P-\tilde{P}^0$ we find that these results are insensitive to E_ν. For instance, a change of E_ν by 0.81 to $E_\nu=0.25$ Ry changes both the total energy and the energy eigenvalue by about 1 mRy. In the MT approximation the errors are substantially larger.

TABLE VI. Results for a truncated proton in jellium with $r_s=4$. The change of the potential is localized to a sphere of radius s^*. The change in the total energy ($\Delta\mathscr{E}$), the position of the bound state (E_b), and the net electronic charge inside the sphere (Δn) are given. The results for $s^*=\infty$ are taken from the calculation of Zaremba *et al.* (Ref. 25).

s^* (a.u.)	$\Delta\mathscr{E}$ (mRy)	E_b (mRy)	Δn (electrons)
1.25	−910	−405	−0.400
1.5	−1024	−421	−0.216
2.0	−1091	−428	0.019
2.5	−1093	−419	0.146
2.982	−1088	−409	0.199
3.5	−1087	−401	0.191
4.5	−1097	−405	0.043
5.0	−1099	−413	−0.036
5.5	−1099	−418	−0.077
∞	−1096	−409	0

We next consider a proton in an otherwise homogeneous electron gas. The calculation is performed as before and the only difference is that we now occupy the bound state doubly and fill the continuum states up to the Fermi energy. We note that, while the perturbation for the free atom decays exponentially, a proton in jellium gives rise to long-range Friedel oscillations. This is illustrated in Table VI where we consider a truncated proton in jellium for which the change of the one-electron potential is localized to a sphere with radius s^*. The net charge inside the sphere,

TABLE VII. Results for a proton in jellium with the fcc lattice structure ($s=2.982$) and including two shells. We have used s, p, and d waves and set $E_\nu=0$, i.e., at the bottom of the continuum. The exact results are those of Zaremba *et al.* (Ref. 25).

	H in jellium			
	$\Delta\mathscr{E}$ (mRy)		E_b (mRy)	
	$r_s=3$	$r_s=4$	$r_s=3$	$r_s=4$
ASA, approximate $\tilde{g}_0$	−1071	−1096	−513	−419
ASA, exact g_0	−1063	−1095	−511	−405
Exact	−1062	−1096	−514	−409

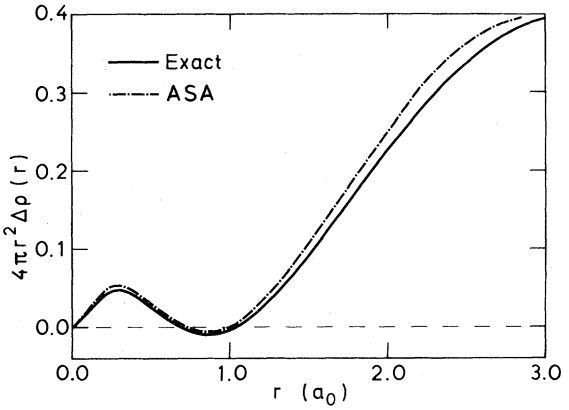

FIG. 2. Induced valence charge density for a lithium ion in an $r_s=4$ jellium. The solid curve shows the exact density (Ref. 25) and the dashed curve shows our density calculated with the LMTO-ASA method. For the jellium we used the fcc structure of Al ($s=2.982$). The perturbation was included in the spheres at the central and nearest-neighbor sites (see also Table VIII).

$$\Delta n = \int_{r\le s*} d^3r\, \Delta n\,(r) - 1\ ,$$

is positive for $s^*\sim 2$–4.5, meaning that the induced screening charge contains more than the single electron which would be needed to screen the proton. Owing to the Friedel oscillations, the quantity Δn oscillates with s^* and it can be fairly different from zero. Thus for $s^*=5$, where the Friedel oscillation has a large amplitude, the result is not as well converged as for a free hydrogen atom (Table IV). On the other hand, for small values of s^* the convergence is faster than for the free hydrogen atom since, in this limit, the net screening charge outside the atomic sphere is smaller.

We now fill space with atomic spheres and use the lattice structure and AS radius of Al as before. As has been emphasized earlier, in the calculations based on the approximate unperturbed Green function we improve the description in the perturbed region by using $\Delta P = P - \tilde{P}^0$. The perturbed Green function is therefore calculated with a somewhat higher accuracy than the unperturbed one. To avoid having this improved description show up as a contribution to the binding energy of the impurity, we perform two calculations: one with the impurity and one without. In the latter calculation, the perturbation is simply $\Delta P = P^0 - \tilde{P}^0$, which is the error of the potential function in the calculation for the unperturbed crystal. The difference in total energy between the two calculations defines our binding energy. The results are shown in Table VII. Although the range of the perturbation is larger than for a free hydrogen atom, the results in Table VII are almost as good as in Table V.

TABLE VIII. Total energy of a lithium atom in jellium minus the energy of the unperturbed jellium. Our results were obtained using the fcc lattice structure ($s=2.982$). We located E_v at the bottom of the continuum and included two shells with s, p, and d waves. The exact results are those of Zaremba *et al.* (Ref. 25).

	Li in jellium	
	$\Delta\mathscr{E}$ (mRy)	
	$r_s=3$	$r_s=4$
ASA, approximate $\tilde{g}_0$	−193	−330
Exact	−232	−385

The charge induced by a proton is fairly localized due to the small size of the hydrogen atom, and a substantial part of the perturbation is localized to the central sphere where it is described exactly. We have, however, also considered a lithium atom in jellium, which gives rise to a very extended perturbation because of the large radius of the Li $2s$ orbital. This is illustrated in Fig. 2 which shows the induced charge density for $r_s=4$. The maximum of $4\pi r^2\Delta n\,(r)$ is located outside the central sphere ($s=2.982$), which contains *less than half* of the induced valence charge. The figure also shows that our calculated ASA charge density inside the central sphere is in fairly good agreement with the exact charge density, although somewhat too large. The total energy is shown in Table VIII and it is seen that the ASA result is about 50 mRy above the correct energy.

Finally we show in Table IX the phase shifts at the Fermi energy, which are directly related to the

TABLE IX. Phase shifts at the Fermi energy for a Li impurity in jellium (see caption of Table VIII).

	Li in jellium			
	$r_s=3$		$r_s=4$	
	$\frac{2}{\pi}\eta_s$	$\frac{6}{\pi}\eta_p$	$\frac{2}{\pi}\eta_s$	$\frac{6}{\pi}\eta_p$
ASA, approximate $\tilde{g}^0$	2.04	1.09	2.27	1.11
Exact	1.99	0.95	2.22	0.84

total induced charge density. The phase shifts are generally a bit too large, which can again be understood in terms of the large charge density, corresponding to more than half an electron, which is located outside but close to the central sphere. If properly taken into account, this charge density would raise the potential in the central cell substantially. The spherical approximation for the charge density in the second shell, however, reduces this effect. Thus in the ASA the potential in the central cell is too negative, the calculated induced charge density is too large, and the total energy is too high.

IV. CONCLUSION

We have developed an LMTO-ASA method for self-consistent impurity calculations using the Green-function technique. Compared with current Gaussian-orbital—pseudopotential methods the advantages of the LMTO-ASA and the KKR methods are that they employ proper radial wave functions and a small basis set with typically nine orbitals per perturbed site. The disadvantages of the two methods are that they imply AS or MT approximations and that relaxations of atomic positions are more difficult to include in these methods due to the long range of the structure constants.

Compared with the KKR approach, the linearization of the band-structure problem in the LMTO method leads to a more efficient and physically transparent way of calculating the Green function for the unperturbed crystal, and the substitution of the MT approximation by the ASA not only simplifies the formalism but also increases the accuracy by allowing for perturbations in the region between the MT spheres. When calculating the total energy using the density-functional formalism, we are careful to take optimal advantage of the variational property of the functional. The resulting accuracy is typically 0.01 Ry and the accuracy of individual one-electron energies is about the same. This, together with the small matrix size and the analytical simplicity of our one-electron Hamiltonian, makes the LMTO-ASA method particularly suited for studying trends and for treating more than one (up to about 30) perturbed sites.

ACKNOWLEDGMENTS

We have enjoyed discussions with B. Segall, P. Vogl, M. Scheffler, and D. Glötzel, who, furthermore, provided certain computer subroutines. We are grateful to E. Zaremba and M. J. Stott for making available to us detailed results not contained in their paper.[25]

APPENDIX A: ASA AND KKR GREEN FUNCTIONS

In (2.22) we expressed the imaginary part of the ASA Green function $G(\vec{r},\vec{r}';E)$ in terms of the imaginary part of the matrix $g_{RL,R'L'}(E)$ and the regular solutions $\phi_{Rl}(E,r_R)$ of the radial Schrödinger equations. We now include the real parts and therefore need, in addition to the regular solutions, those solutions, $\phi^{\rm irr}_{Rl}(E,r_R)$, of the radial equations which are irregular at $r_R=0$. As a result of this development our understanding of the relation (2.39) between the matrices g and G will be improved.

The expression for the Green function that we seek could be obtained[15] from the well-known[3,26] KKR Green function by substituting the MT spheres by space-filling atomic spheres and by letting κ^2 tend to zero neglecting the KKR relation (1.4). However, in the KKR formalism the normalizations used for the wave functions are appropriate in a scattering situation but inconvenient in a condensed system where the region inside rather than outside the atoms is of most relevance. We will therefore derive the ASA expression for the Green function directly, using the partial waves and MT orbitals defined in the previous sections. In contrast to what was done there we shall not set κ^2 equal to zero but keep it unspecified. This has the advantages that our formalism includes the KKR formalism and that it illustrates the LMTO-ASA formalism with a general (energy-independent) κ^2. With a negative κ^2, for instance, the structure constants decrease exponentially with interatomic distance.[17] In addition to the traditional partial-wave one-center expansion of the Green function, our derivation yields a MT orbital multicenter expansion with superior convergence.

The Green function is defined by (1.3) and $V(\vec{r})$ is an AS potential, as defined in (2.4); it extends to infinity but does not necessarily have crystalline symmetry. The source point $\vec{r}'$ lies inside a sphere whose center we name $\vec{R}'$. That is $r'_{R'}\equiv|\vec{r}'-\vec{R}'|\leq s_{R'}$. Considered a function of the field point $\vec{r}$, a solution $G(\vec{r},\vec{r}'_{R'}+\vec{R}';E)$ of (1.3) may be expressed as a linear combination of the regular Schrödinger solutions $\phi_{R'L}(E,\vec{r}_{R'})$ when $\vec{r}\equiv\vec{r}_{R'}+\vec{R}'$ lies inside the R' sphere and inside the source point, as a linear combination of the irregular Schrödinger solutions $\phi^{\rm irr}_{R'L}(E,\vec{r}_{R'})$ when $\vec{r}$ lies in the R' sphere but outside the source point, and as a linear combination of the regular Schrödinger solutions $\phi_{RL}(E,\vec{r}_R)$ when $\vec{r}$ lies in a sphere centered at $\vec{R}\neq\vec{R}'$. Taking the symmetry of G with respect to an interchange of $\vec{r}$ and $\vec{r}'$ into account, we thus arrive at the well-known form

$$G(\vec{r}_R+\vec{R},\vec{r}'_{R'}+\vec{R}';E)=\delta_{RR'}\sum_L \phi_{RL}(E,\vec{r}_R^<)W_{Rl}(E)^{-1}\phi_{RL}^{\rm irr}(E,\vec{r}_R^>)$$
$$+\sum_L\sum_{L'}\phi_{RL}(E,\vec{r}_R)G_{RL,R'L'}(E)\phi_{R'L'}(E,\vec{r}'_{R'}) , \tag{A1}$$

where $\vec{r}_R^<$ is the smaller, and $\vec{r}_R^>$ the larger, of $\vec{r}_R$ and $\vec{r}'_R$. Expression (A1) is a one-center expansion for the Green function, analogous to the expansion (2.10) for the wave function, and the coefficients W and G must now be determined in such a way that (A1) satisfies (1.3) and that the expansions around the various sites match together.

The second term of (A1) is a general solution of the homogeneous (i.e., the Schrödinger) equation, and in order that the first term be a particular solution of the inhomogeneous equation (1.3), W must be equal to the Wronskian, i.e.,

$$W(E)=W\{\phi(E),\phi^{\rm irr}(E)\}\equiv r^2\left[\phi(E,r)\frac{\partial\phi^{\rm irr}(E,r)}{\partial r}-\phi^{\rm irr}(E,r)\frac{\partial\phi(E,r)}{\partial r}\right]$$
$$=s\phi(E,s)\phi^{\rm irr}(E,s)[D^{\rm irr}(E)-D(E)] . \tag{A2}$$

This follows from Gauss's theorem. The Wronskian is independent of r because ϕ and $\phi^{\rm irr}$ satisfy the same radial Schrödinger equation. In (A2) we have for simplicity of notation dropped the subscripts R and l.

Using (A2) we see that the first term of (A1) is independent of the multiplicative normalizations of ϕ and $\phi^{\rm irr}$. The first term does, however, depend on the additive normalization of $\phi^{\rm irr}$: Given an irregular solution, $\phi^{\rm irr}$, we may obtain another one by adding some constant times ϕ to it whereby the corresponding new first term of the Green function differs from the old one by a solution of the homogeneous equation. This solution may be absorbed into the diagonal part of the second term of (A1) and the entire Green function remains unaltered. Specifically, for the two irregular solutions $\phi^a(E,r)$ and $\phi^b(E,r)$, characterized by the respective logarithmic derivatives $D^a(E)$ and $D^b(E)$ $[\neq D(E)]$, we have

$$\frac{1}{D^a-D}\frac{\phi^a(r)}{\phi^a(s)}=\frac{1}{D^b-D}\frac{\phi^b(r)}{\phi^b(s)}+\left[\frac{1}{D^a-D}-\frac{1}{D^b-D}\right]\frac{\phi(r)}{\phi(s)} , \tag{A3}$$

as may be checked by setting $r=s$ and by performing the radial derivative at s. In (A3) we have dropped the argument E as well as the subscripts R and l. For use in (A1), therefore,

$$\phi(\vec{r}^<)(W\{\phi,\phi^a\})^{-1}\phi^a(\vec{r}^>)=\phi(\vec{r}^<)(W\{\phi,\phi^b\})^{-1}\phi^b(\vec{r}^>)+\phi(\vec{r})\frac{W\{\phi^a,\phi^b\}}{W\{\phi,\phi^a\}W\{\phi,\phi^b\}}\phi(\vec{r}') . \tag{A4}$$

In order to determine the coefficients $G_{RL,R'L'}$, we shall set up a MTO expansion for the Green function analogous to what we did in Sec. II A and require that it equals the one-center expansion (A1). This is, in fact, equivalent to using a Dyson equation with

$$G^{00}(\vec{r}-\vec{r}';\kappa^2)=-\frac{\exp(-i\kappa|\vec{r}-\vec{r}'|)}{4\pi|\vec{r}-\vec{r}'|} , \quad {\rm Im}\kappa\leq 0 \tag{A5}$$

and the perturbation $E-V(r)-\kappa^2$. In terms of this free-electron Green function the MTO may be defined as

$$\chi_{RL}(\kappa^2,E,\vec{r}-\vec{R})\equiv-\int_R d^3r'G^{00}(\vec{r}-\vec{r}';\kappa^2)[E-V(r')-\kappa^2]\phi_{RL}(E,\vec{r}'-\vec{R}) , \tag{A6}$$

where the integral in the sphere at R may be solved by using (1.1) together with Green's second identity and the well-known one-center expansion

$$G^{00}(\vec{r}-\vec{r}';\kappa^2)=\sum_L j_L(\vec{r}^<)\kappa h_L(\vec{r}^>) . \tag{A7}$$

This expansion is a special case of (A1) where the regular functions

$$j_L(\vec{r})\equiv j_l(\kappa r)Y_L(\hat{r})$$

and the irregular functions

$$i\kappa h_L(\vec{r})\equiv i\kappa h_l(\kappa r)Y_L(\hat{r})\equiv\kappa[n_l(\kappa r)+ij_l(\kappa r)]Y_L(\hat{r})$$

are related to the spherical Bessel functions j_l, Neumann functions n_l, and Hankel functions h_l, as indicated. The Wronskian, as defined in (A2), satisfies

$$W\{j_l,i\kappa h_l\}=W\{j_l,\kappa n_l\}=1\ . \tag{A8}$$

The result for the MTO is

$$\chi_{RL}(\kappa^2,E,\vec{r}_R)=\begin{cases}\phi_{RL}(E,\vec{r}_R)+j_L(\vec{r}_R)W\{i\kappa h_l,\phi_{Rl}\} & \text{for } r_R\le s_R\\ i\kappa h_L(\vec{r}_R)W\{j_l,\phi_{Rl}\} & \text{for } r_R\ge s_R\end{cases} \tag{A9}$$

where the Wronskians should be evaluated at the sphere ($r_R=s_R$). Equation (A9) reduces to (2.11) in the limit of vanishing κ^2 because

$$j_l(\kappa r)\to\frac{(\kappa r)^l}{(2l+1)!!},\quad ih_l(\kappa r)\to\frac{(2l-1)!!}{(\kappa r)^{l+1}} \tag{A10}$$

in that limit. We may now, as we did in (2.12), expand the tail of the MTO centered at $\vec{R}$ in the sphere centered at $\vec{R}'$ ($\neq\vec{R}$) using the addition theorem

$$\begin{aligned}i\kappa h_L(\vec{r}_R)&=\sum_{L'}j_{L'}(\vec{r}_{R'})\sum_{l''}4\pi C_{LL'L''}i^{-l+l'-l''}i\kappa h_{L''}(\vec{R}-\vec{R}')\\&\equiv\sum_{L'}j_{L'}(\vec{r}_{R'})\mathscr{B}_{R'L',RL}\quad\text{for }\vec{R}\neq\vec{R}'\ .\end{aligned} \tag{A11}$$

Here

$$C_{LL'L''}\equiv\int d\hat{r}\,Y_L\,Y^*_{L'}\,Y_{L''}$$

are the Gaunt coefficients such that $m''=m'-m$ and the l'' summation includes only the terms with

$$l''=|\,l'-l\,|\,,|\,l'-l\,|+2,\ldots,(l'+l)\ .$$

The matrix $\mathscr{B}$ is the KKR structure matrix.[26] We may finally express the MTO as one-center expansions using vector notation as in (2.14); the result is

$$|\,\phi\rangle+|\,j\rangle\left[\frac{W\{i\kappa h,\phi\}}{W\{j,\phi\}}+\mathscr{B}\right]W\{j,\phi\}=|\,\chi\rangle^{\infty}\ . \tag{A12}$$

Here the Wronskians are regarded as diagonal matrices and, for $\kappa^2=E-V_{\mathrm{MTZ}}$, the relation to the phase shifts η^0 is

$$\frac{W\{i\kappa h,\phi\}}{W\{j,\phi\}}=\kappa\left[\frac{W\{n,\phi\}}{W\{j,\phi\}}+i\right]=\kappa(\cot\eta^0+i)\ . \tag{A13}$$

The values of κ^2 most relevant for LMTO calculations are negative or zero. For these values the free-electron Green function (A5) and the MTO's (A6) are real, but the Bessel and Hankel functions of odd order are imaginary and behave similar to (A10) in the limit of vanishing κ. We shall therefore renormalize the Bessel and Hankel functions such that they become real for $\kappa^2\le 0$ and, for $\kappa^2=0$, reduce to the functions used in Sec. II. The regular function

$$J_l(r)\equiv\tfrac{1}{2}[(2l-1)!!](\kappa a)^{-l}j_l(\kappa r) \tag{A14}$$

is real for all real κ^2 and reduces to $[2(2l+1)]^{-1}(r/a)^l$ for $\kappa^2=0$. Here a is an arbitrary linear dimension of the structure as in Sec. II. The irregular function

$$K_l(r)\equiv-[(2l-1)!!(\kappa a)^{-l}]^{-1}ia\kappa h_l(\kappa r) \tag{A15}$$

is real and decreases asymptotically like $r^{-1}\times\exp(-|\,\kappa\,|\,r)$ when κ^2 is negative. For $\kappa^2=0$ it reduces to $(a/r)^{l+1}$. The Wronskian satisfies

$$W\{J_l,K_l\}=-a/2\ . \tag{A16}$$

In terms of J and K the expression (A9) for the MTO may be written as

$$\chi_{RL}(\kappa^2,E,\vec{r}_R)=\begin{cases}\phi_{RL}(E,\vec{r}_R)+J_L(\vec{r}_R)W\{K_l,\phi_{Rl}\}(-2/a) & \text{for } r_R\le s_R\\ K_L(\vec{r}_R)W\{J_l,\phi_{Rl}\}(-2/a) & \text{for } r_R\ge s_R\end{cases} \tag{A17}$$

and the expression (A12) as

$$|\phi\rangle+|J\rangle(P-S)W\{J,\phi\}(-2/a)=|\chi\rangle^{\infty}\ , \tag{A18}$$

with

$$S_{R'L',RL}\equiv\frac{(a/2)\mathscr{B}_{R'L',RL}}{\frac{1}{2}[(2l'-1)!!](\kappa a)^{-l'}\frac{1}{2}[(2l-1)!!](\kappa a)^{-1}}$$

$$=\sum_{l''}(-1)^{l+1}(i\kappa a)^{l+l'-l''}4\pi C_{LL'L''}\frac{2[(2l''-1)!!]}{[(2l'-1)!!][(2l-1)!!]}K_{L''}(\vec{R}-\vec{R}\,') \tag{A19}$$

and

$$P_{Rl}(E)\equiv\frac{W\{K_l,\phi_{Rl}(E)\}}{W\{J_l,\phi_{Rl}(R)\}}\ . \tag{A20}$$

Moreover, by differentiation of (A20) and use of (2.16) we find that

$$\dot{P}_{Rl}(E)=(a/2)[W\{J_l,\phi_{Rl}(E)\}]^{-2}\ , \tag{A21}$$

whereby $\dot{P}^{-1/2}(2/a)^{1/2}=W\{J,\phi\}(-2/a)$, which defines the sign of $\dot{P}^{1/2}$. It is easily checked that expressions (A17)—(A21) reduce to those given in Sec. II when $\kappa=0$.

We are finally in the position to determine the coefficients $G_{RL,R'L'}(E)$ of the one-center expansion (A1) for the Green function. We first assume that $W\{\phi,\chi\}\neq 0$ and choose for the irregular solutions of the radial Schrödinger equation $\phi^{\rm irr}$ those functions which match continuously and differentiably onto the corresponding MTO's χ at the sphere. These functions we call ϕ^{χ} and the corresponding expansion coefficients G^{χ}. Equation (A1) thus reads

$$G(\vec{r}_R+\vec{R},\vec{r}\,'_{R'}+\vec{R}\,';E)=\delta_{RR'}\sum_L\phi^{\chi}_{RL}(E,\vec{r}\,^{>}_R)\dot{P}_{Rl}(E)[P_{Rl}(E)]^{-1}\phi_{RL}(E,\vec{r}\,^{<}_R)$$

$$+\sum_L\sum_{L'}\phi_{RL}(E,\vec{r}_R)G^{\chi}_{RL,R'L'}(E)\phi_{R'L'}(E,\vec{r}\,'_{R'})\ , \tag{A22}$$

where we have used that, according to (A9) or (A17), (A20), and (A21),

$$W\{\phi,\phi^{\chi}\}=W\{\phi,\chi\}=W\{\phi,i\kappa h\}W\{j,\phi\}=W\{\phi,K\}W\{J,\phi\}(-2/a)=P\dot{P}^{-1}\ . \tag{A23}$$

Let us now keep that coordinate $\vec{r}\,'$ which lies closest to a site ($\equiv\vec{R}\,'$) fixed and determine the coefficients G by demanding that the Green function $G(\vec{r},\vec{r}\,';E)$, obtained by summing (A22) over all R, is a smooth function of the other coordinate $\vec{r}$. In (A22) we thus have $\vec{r}^{\,>}=\vec{r}$ and $\vec{r}^{\,<}=\vec{r}\,'$.

We may require that (A22) summed over all R is identical to the following multicenter expansion of overlapping MTO's:

$$G(\vec{r},\vec{r}\,'_{R'}+\vec{R}\,';E)\equiv\sum_{L'}\chi^{\rm irr}_{R'L'}(E,\vec{r}\,'_{R'})\dot{P}_{R'l'}(E)[P_{R'l'}(E)]^{-1}\phi_{R'L'}(E,\vec{r}\,'_{R'})$$

$$+\sum_{R,L}\sum_{L'}\chi_{RL}(E,\vec{r}_R)G^{\chi}_{RL,R'L'}(E)\phi_{R'L'}(E,\vec{r}\,'_{R'})\ , \tag{A24}$$

which, by construction, is a smooth function of $\vec{r}$. Here χ is the usual MTO given by one of the equivalent expressions (A6), (A9), or (A17) and $\chi^{\rm irr}$ is a continuous and differentiable function in all space; it equals the irregular function ϕ^{χ} inside the sphere and the MTO outside the sphere. In other words, it is a MTO augmented continuously and differentiably inside the sphere by the appropriate irregular solution of Schrödinger's equation. We now project (A24) onto $\phi_{R'L'}(E,\vec{r}\,'_{R'})$ and express the $\vec{r}$ dependence by one-center expansions using the expansion (A11) or (A18) of the MTO tail. With vector notation (A24) becomes

$$|\chi^{\rm irr}\rangle\infty\dot{P}P^{-1}+|\chi\rangle\infty G^{\chi}=|\phi^{\chi}\rangle\dot{P}P^{-1}-|J\rangle S(2/a)^{1/2}\dot{P}^{1/2}P^{-1}$$
$$+|\phi\rangle G^{\chi}+|J\rangle(P-S)\dot{P}^{-1/2}(2/a)^{1/2}G^{\chi}\ ,$$

while (A22), summed over R, yields

$$|\phi^{\chi}\rangle\dot{P}P^{-1}+|\phi\rangle G^{\chi}\ .$$

The condition that the two expressions are identical is

$$S\dot{P}^{1/2}P^{-1}=(P-S)\dot{P}^{-1/2}G^{\chi}\ ,$$

which yields the wanted relation

$$G^{\chi}(E)=[\dot{P}(E)]^{1/2}[g(E)-P(E)^{-1}][\dot{P}(E)]^{1/2} \tag{A25}$$

between the coefficients of the Green-function expansions (A22) and (A24) and the matrix $\underline{g}=(\underline{P}-\underline{S})^{-1}$. By taking the imaginary part and comparing with (2.22) we realize that for the poles of $P(E)$ and $P(E)^{-1}$ the principal parts should be taken. In KKR notation (A25) becomes

$$G^{\chi}(E)=-(W\{j,\phi\})^{-1}[(\kappa\cot\eta^{0}+i\kappa+\mathscr{B})^{-1}-(\kappa\cot\eta^{0}+i\kappa)^{-1}](W\{j,\phi\})^{-1}\ , \tag{A26}$$

as obtained by using (A12) instead of (A18).

The term $-\dot{P}(E)[P(E)]^{-1}$ in the diagonal of (A25) and (A26) contains the factor $W\{K,\phi(E)\}^{-1}$, as may be seen from (A13) and (A20). The corresponding pole is, of course, not present in the Green function (A22) and it may be removed by rearrangement of the terms in (A22): If the term $-\phi(r)\dot{P}P^{-1}$ from the diagonal of the second term in (A22) is combined with the term $\phi^{\chi}(r)\dot{P}P^{-1}$ we obtain $\phi^{J}(r)(W\{\phi,J\})^{-1}$, where $\phi^{J}(r)$ is the irregular solution which matches continuously and differentiably onto $J(r)$ at the sphere [see Eqs. (A17) and (A23)]. As a result, the Green function is given by (A1) and (A2) with $\phi^{\rm irr}(r)=\phi^{J}(r)$ and with the coefficients

$$G^{J}(E)=[\dot{P}(E)]^{1/2}g(E)[\dot{P}(E)]^{1/2} \tag{A27}$$
$$=-(W\{j,\phi\})^{-1}(\kappa\cot\eta^{0}+i\kappa+\mathscr{B})^{-1}(W\{j,\phi\})^{-1}\ . \tag{A28}$$

For the poles caused by the presence of the factors $(W\{\phi(E),J\})^{-1}$ in the first term of (A1) as well as in (A27) and (A28), the principal parts should be taken.

The general expressions for the coefficients $G(E)$ and $W(E)^{-1}$ in (A1) are

$$G(E)=\mathscr{P}\frac{W\{J,\phi^{\rm irr}(E)\}}{W\{J,\phi(E)\}W\{\phi^{\rm irr}(E),\phi(E)\}}+G^{J}(E) \tag{A29}$$

and

$$[W(E)]^{-1}=-\mathscr{P}[W\{\phi^{\rm irr}(E),\phi(E)\}]^{-1}\ , \tag{A30}$$

as obtained by starting out from (A27) and using (A4) and (A2). So far we have considered the special choices $\phi^{\rm irr}=\phi^{\chi}$ and $\phi^{\rm irr}=\phi^{J}$. The Green function $G(\vec{r},\vec{r}';E)$ has poles at the eigenvalues of Schrödinger's equation for the entire system only, and any additional poles such as those caused by the factors $[W\{\phi^{\rm irr}(E),\phi(E)\}]^{-1}$ and $[W\{J,\phi(E)\}]^{-1}$ present in the various parts of the one-center expansion (A1) must cancel. It is now customary to specify that the first term of (A1), and hence (A30), has no poles. [Strictly speaking, *only* those choices of $\phi^{\rm irr}$ for which $W\{\phi^{\rm irr},\phi(E)\}\neq 0$ for all E are possible. This is so because if for some energy we had chosen $D^{\rm irr}=D(E)$, then the solution of the radial Schrödinger equation for that energy and that boundary condition would contain *no* irregular part.] We must thus choose some radial function whose logarithmic derivative never equals $D(E)$ and then match $\phi^{\rm irr}$ onto that function.

In the ASA we specify [see (2.7)] that ϕ is normalized to unity in its sphere and, as a consequence, ϕ is orthogonal to its energy-derivative function $\dot{\phi}$. Moreover, the Wronskian of these two functions take the value 1 at the sphere as shown in Sec. II B. In the ASA a natural choice for the irregular solution is therefore the function $\dot{\phi}$ which matches onto $\dot{\phi}$. If with this choice we now use (A29) and (A30) together with (A21) we realize that

$$G^{\cdot}(E)=\mathscr{P}\left[-\frac{1}{2}\frac{d\ln\dot{P}(E)}{dE}\right]+G^{J}(E) \tag{A31}$$

and

$$[W^{\cdot}(E)]^{-1}=-1\ . \tag{A32}$$

Since neither the first term of (A1) nor the functions ϕ have any poles, the coefficients $G_{RL,R'L'}(E)$ must have exactly the same poles as $G(\vec{r},\vec{r}';E)$. This has the consequence that the pole caused by the presence of the factor $[W\{J,\phi(E)\}]^{-1}$ in the first term of (A31) must cancel an identical pole of $G^J(E)$. Furthermore, if we neglect the geometry violation of the ASA, the Green function $G(\vec{r},\vec{r}';E)$ and herewith $G^{\cdot}(E)$ cannot depend on κ. We may therefore take $\kappa=0$. If we finally substitute in (A31) the appropriate second-order form (2.34) for $[\dot{P}(E)]^{-1/2}$ and compare with (2.39) we realize that

$$\widetilde{G}^{\cdot}(E)=\widetilde{G}(E)\ , \tag{A33}$$

as defined in (2.38). This is an important result.

For certain applications it is practical to have exponentially decreasing structure constants and therefore to use a (slightly) negative κ^2. In order to calculate $\widetilde{G}^{\cdot}(E)=(E-i0^+-H)^{-1}$ we need an expression analogous to (2.3) for the Hamiltonian but valid for a general κ. From the development given in Sec. II B we may see that (2.3) does, in fact, hold for a general κ provided that S is given by (A19), that $P(E)$ is given by (A20), and that in the definitions (2.32) of the potential parameters the radial functions with logarithmic derivatives l and $-l-1$ should be substituted by, respectively $J_l(r)$ and $K_l(r)$.

In the KKR formalism ϕ and $\phi^{\rm irr}$ are normalized according to their behavior *at* and *outside* the sphere. The linearly independent functions used for the construction of the boundary condition for $\phi^{\rm irr}$ are not ϕ and $\dot{\phi}$ as in the ASA formalism but $j_l(\kappa r)$ and $n_l(\kappa r)$ whose Wronskian equals κ^{-1} [Eq. (A8)]. The multiplicative normalization of ϕ is such that

$$\phi(r)=\cos\eta^0 j(r)-\sin\eta^0 n(r) \tag{A34}$$

when $r\geq s$. With this normalization,

$$W\{\phi,j\}=\kappa^{-1}\sin\eta^0$$

and (A35)

$$W\{\phi,n\}=\kappa^{-1}\cos\eta^0\ .$$

The choice for the boundary condition of $\phi^{\rm irr}$

$$\phi^{\rm irr}(r)=\sin\eta^0 j(r)+\cos\eta^0 n(r) \tag{A36}$$

therefore leads to $W\{\phi,\phi^{\rm irr}\}=\kappa^{-1}$, which always differs from zero. With these κ-dependent normalizations the coefficients (A29) and (A30) in the one-center expansion (A1) of the Green function become

$$G^{\rm KKR}(E)=\mathscr{P}\kappa\cot\eta^0+G^J(E) \tag{A37}$$

and

$$[W^{\rm KKR}(E)]^{-1}=\kappa\ . \tag{A38}$$

In the present Appendix the ASA has amounted to using the expansion (A11) of the MTO beyond its range of validity as if the atomic spheres did not overlap. If, specifically, the MTO centered at site $\vec{R}$ is expanded about site $\vec{R}'$, then the expansion *converges* inside the (large) sphere which is centered at $\vec{R}'$ and passes through $\vec{R}$ and has the radius $\vec{R}-\vec{R}'$. The *result* of the expansion applies to the *tail* of MTO, however, and is consequently correct only inside that part of the large sphere which lies outside the atomic sphere centered at $\vec{R}$. If now $\vec{R}$ and $\vec{R}'$ are nearest neighbors, the expansion is seldomly correct *throughout* the atomic sphere centered at $\vec{R}'$. When the potential has the MT form it is not necessary (although convenient) to use the ASA because the choice $\kappa^2=E-V_{\rm MTZ}$ makes the perturbation used in (A6) vanish outside the nonoverlapping MT spheres and, in that case, the MTO expansions hold throughout all MT spheres. This is the basis for the KKR method.

We finally study the l convergence of the one-center (A1) and multicenter (A24) expansions of the Green function. For increasing values of l the centrifugal term $l(l+1)r^{-2}$ dominates the radial Schrödinger equation, and the radial wave functions ϕ_l approach the spherical Bessel functions j_l or J_l, and eventually they approach r^l. Therefore, in order to study the convergence, we need only consider the case of free electrons. In this case the potential functions (A20) diverge such that

$$g\equiv(P-S)^{-1}=P^{-1}+P^{-1}SP^{-1}\ , \tag{A39}$$

and, according to (A25) and (A20) and (A21),

$$G^{\chi}=\dot{P}^{1/2}P^{-1}SP^{-1}\dot{P}^{1/2}=\frac{2}{a}\frac{J(s)}{\phi(s)}S\frac{J(s)}{\phi(s)}\ , \tag{A40}$$

which is, essentially, the structure matrix.

For free electrons the one-center expansion (A1) or (A22) becomes

$$G(\vec{r}_R+\vec{R},\vec{r}'_{R'}+\vec{R}';E)=\delta_{RR'}\sum_L J_L(E,\vec{r}_R^{<})(-2/a)K_L(E,\vec{r}_R^{>})$$
$$+(2/a)\sum_L\sum_{L'}J_L(E,\vec{r}_R)S_{RL,R'L'}(E)J_{L'}(E,\vec{r}'_{R'})\ , \tag{A41}$$

where we have used (A40) and the argument $\kappa^2=E$ of the Bessel and Hankel functions. Moreover, $S_{R=R'}\equiv 0$. The one-center expansion thus reduces, as it should, to the result that could have been obtained directly by combination of (A11) with (A7). We shall now see that the one-center expansion converges unconditionally inside the MT spheres and not further.

For $E=0$ the *first* term becomes

$$\delta_{RR'}\sum_L J_L(\vec{r}_R^{<})(-2/a)K_L(\vec{r}_R^{>})=(-4\pi)^{-1}\delta_{RR'}\sum_l P_l(\hat{r}_R\cdot\hat{r}'_R)r_R^{<l}/r_R^{>l+1}\ , \tag{A42}$$

where we have used (A14) and (A15) and the addition theorem $4\pi\sum_m Y_L(\hat{r})Y_L(\hat{r}')=(2l+1)P_l(\hat{r}\cdot\hat{r}')$. Here P_l is a Legendre polynomial. Since $|P_l|\leq 1$ the series (A42) converges for $r_R^{<}<r_R^{>}$.

If, in the *second* term of (A42) we perform the L summation before the L' summation, we obtain

$$(2/a)\sum_{L'}\left[\sum_L J_L(\vec{r}_R)S_{RL,R'L'}\right]J_{L'}(\vec{r}'_{R'})=\sum_{L'}K_{L'}(\vec{r}_{R'})(-2/a)J_{L'}(\vec{r}'_{R'})\ =(4\pi)^{-1}\sum_{l'}P_{l'}(\hat{r}'_{R'}\cdot\hat{r}_{R'})(r'_{R'})^{l'}/(r_{R'})^{l'+1} \tag{A43}$$

with the help of the expansion theorem (A11) or (A18). Since there is no value of the angle between $\vec{r}_{R'}$ and $\vec{r}'_{R'}$ for which $P_{l'}$ tends to zero as l' tends to infinity, the series (A43) converges for $r'_{R'}<r_{R'}$ and it *diverges* for $r'_{R'}>r_{R'}$. If instead we perform the L' summation before the L summation, the result converges for $r_R<r'_R$ and it *diverges* for $r_R>r'_R$. This means that the real part of the one-center expansion (A1) of the Green function converges unconditionally only for $\vec{r}$ and $\vec{r}'$ inside the nonoverlapping MT spheres. This expansion is therefore not useful for the treatment of non-MT or non-ASA perturbations.

We now consider the multi-center MTO expansion (A24). The MTO vanishes for free electrons due to the presence of the factor $W\{j,\phi\}$ in (A9) and, as a result, the second term of the multicenter expansion (A24) vanishes. The first term remains because, according to (A9),

$$\chi^{\rm irr}(\vec{r})=i\kappa h(\vec{r})W\{j,\phi\}\ ,$$

and $\dot{P}P^{-1}$ is given by (A23). The multicenter expansion thus reduces to (A7), as it should, *and it converges for all r and r', except for r=r'.*

APPENDIX B: FREE-ELECTRON GREEN FUNCTION IN THE ASA

For the case of free electrons it is possible to give an exact expression for the Green-function matrix $g(E)\equiv[P(E)-S]^{-1}$ which neither contains the geometry violation of the ASA nor the errors caused by the parametrization of the potential functions, nor a matrix inversion. If we make the KKR choice $\kappa^2=E$ the result is, of course, given by (A39). We shall, however, choose $\kappa^2=0$ and therefore obtain the corresponding $g(E)$ by comparing the ASA free-electron Green function obtained from (A1) with the exact result (A41). For free electrons $\phi(E,r)=J(E,r)\langle J(E)^2\rangle^{-1/2}$, and (A1) yields

$$\begin{aligned}G(\vec{r}_R+\vec{R},\vec{r}'_{R'}+\vec{R}';E)=&\delta_{RR'}\sum_L J_{RL}(E,\vec{r}_R^{<})[W\{J(E),\phi^{J(0)}(E)\}]^{-1}\phi_{RL}^{J(0)}(E,\vec{r}_R^{>})\\&+\sum_L\sum_{L'}J_{RL}(E,\vec{r}_R)\langle J_{Rl}^2\rangle^{-1/2}G_{RL,R'L'}^{J(0)}(E)\langle J_{R'l'}^2\rangle^{-1/2}J_{R'L'}(E,\vec{r}'_{R'})\ .\end{aligned} \tag{B1}$$

The irregular solution is a linear combination of the spherical Bessel and Hankel functions $J(E)$ and $K(E)$ with $\kappa^2=E$, and we have specifically chosen $D^{\rm irr}=D^{J(0)}=l$. Here $J(0)$ is the spherical Bessel function with $\kappa^2=0$. The relation to g is given by (A27) and (A21), i.e.,

$$\langle J(E)^2\rangle^{-1/2}G^{J(0)}(E)\langle J(E)^2\rangle^{-1/2}=(a/2)[W\{J(0),J(E)\}]^{-1}g(E)[W\{J(0),J(E)\}]^{-1}\ . \tag{B2}$$

In order to compare (B1) with (A41) we rearrange the terms of the latter using (A4) with $\phi^a\equiv K(E)$, $\phi^b\equiv\phi^{J(0)}(E)$, and $\phi=J(E)$. The result of the comparison is then that (B2) must equal

$$\frac{W\{K(E),\phi^{J(0)}(E)\}}{W\{J(E),K(E)\}W\{J(E),\phi^{J(0)}(E)\}}+\frac{2}{a}S(E)\ ,$$

where the structure matrix with $\kappa^2=E$ was given in (A19). Since $\phi^{J(0)}(E)$ matches onto $J(0)$ and $W\{J,K\}=-a/2$, the final result is

$$g(E)=\frac{4}{a^2}W\{J(E),J(0)\}\left[S(E)-\frac{W\{K(E),J(0)\}}{W\{J(E),J(0)\}}\right]W\{J(E),J(0)\}\ . \tag{B3}$$

[1]J. Bernholc and S. T. Pantelides, Phys. Rev. B 18, 1780 (1978); J. Bernholc, N. O. Lipari, and S. T. Pantelides, Phys. Rev. Lett. 41, 895 (1978); Phys. Rev. B 21, 3545 (1980); N. O. Lipari, J. Bernholc, and S. T. Pantelides, Phys. Rev. Lett. 43, 1354 (1979); J. Bernholc, S. T. Pantelides, N. O. Lipari; and A. Baldareschi, Solid State Commun. 37, 705 (1981); M. Scheffler, S. T. Pantelides, N. O. Lipari, and J. Bernholc, Phys. Rev. Lett. 47, 413 (1981).

[2]G. A. Baraff and M. Schlüter, Phys. Rev. Lett. 41, 892 (1978); G. A. Baraff, E. O. Kane, and M. Schlüter, Phys. Rev. B 21, 3563 (1980); G. B. Bachelet, G. A. Baraff, and M. Schlüter, *ibid.* 24, 915 (1981); 24, 4736 (1981); M. Lannoo, G. A. Baraff, and M. Schlüter, *ibid.* 24, 955 (1981).

[3]R. Zeller and P. H. Dederichs, Phys. Rev. Lett. 42, 1713 (1979); R. Zeller, R. Podloucky, and P. H. Dederichs, Z. Phys. B 38, 165 (1980); R. Podloucky, R. Zeller, and P. H. Dederichs, Phys. Rev. B 22, 5777 (1980); J. Deutz, P. H. Dederichs, and R. Zeller, J. Phys. F 11, 1787 (1981); P. H. Dederichs and R. Zeller, in *Festkörperprobleme (Advances in Solid State Physics)*, edited by J. Treusch (Vieweg, Braunschweig, 1981), Vol. XXI, p. 243.

[4]See, e.g., H. P. Hjalmarson, P. Vogl, D. J. Wolford, and J. D. Dow, Phys. Rev. Lett. 44, 810 (1980); P. Vogl, in *Festkörperprobleme (Advances in Solid State Physics)*, edited by J. Treusch (Vieweg, Braunschweig, 1981), Vol. XXI, p. 191.

[5]O. K. Anderson, Solid State Commun. 13, 133 (1973); Phys. Rev. B 12, 3060 (1975); the latter paper contains the equations referred to in the text. O. K. Andersen and O. Jepsen, Physica 91B, 317 (1977).

[6]H. L. Skriver, *The LMTO Method* (Springer, Heidelberg, 1983).

[7]O. K. Andersen, Europhys. News 12 (5),4 (1981); *The Electronic Structure of Complex Systems*, edited by P. Phariseau (Plenum, New York, 1983), O. K. Andersen and O. Jepsen (unpublished); D. Glötzel, O. K. Andersen, and O. Jepsen, Adv. Phys. (in press).

[8]See, e.g., D. G. Pettifor, J. Phys. F 7, 613 (1977); 8, 219 (1978).

[9]See, e.g., A. R. Mackintosh and O. K. Andersen, in *Electrons at the Fermi-surface*, edited by M. Springford (Cambridge University Press, New York, 1980) and references therein.

[10]See, e.g., G. D. Watkins and R. P. Messmer, Phys. Rev. Lett. 25, 656 (1970); G. G. DeLeo, G. D. Watkins, and W. B. Fowler, Phys. Rev. B 23, 1851 (1981), and references therein.

[11]See, e.g., S. G. Louie, M. Schlüter, J. R. Chelikowsky, and M. L. Cohen, Phys. Rev. B 13, 1654 (1976).

[12]G. F. Koster and J. C. Slater, Phys. Rev. 94, 1392 (1954); 95, 1165 (1954).

[13]J. Callaway, J. Math. Phys. 5, 783 (1964); Phys. Rev. 154, 515 (1967).

[14]J. Callaway and A. Huges, Phys. Rev. 156, 860 (1967); F. Bassani, G. Iadonisi, and B. Preziosi, *ibid.* 186, 735 (1969); M. Jaros and S. Brand, Phys. Rev. B 14, 4494 (1976); C. Koenig and E. Daniel, J. Phys. (Paris) 42, L193 (1981); C. Koenig, P. Léonard, and E. Daniel, *ibid.* 42, 1015 (1981).

[15]This technique has also been applied in many other contexts, such as chemisorption: O. Gunnarsson, H. Hjelmberg, and B. I. Lundqvist, Phys. Rev. Lett. 37, 292 (1976).

[16]O. Gunnarsson, J. Harris, and R. O. Jones, Phys. Rev. B 15, 3027 (1977); J. Harris, in *The Electronic Structure of Complex Systems*, edited by P. Phariseau (Plenum, New York, 1983), O. K. Andersen and R. G. Wolley, Mol. Phys. 26, 905 (1973).

[17]U. Lindefelt and A. Zunger, Phys. Rev. B 24, 5913 (1981); A. R. Williams, P. J. Feibelman, and N. D. Lang, *ibid.* 26, 5433 (1982); G. A. Baraff, M. Schlüter, and G. Allen, *ibid.* 27, 1010 (1983).

[18]D. Glötzel, B. Segall, and O. K. Andersen, Solid State Commun. 36, 403 (1980).

[19]See, e.g., O. Gunnarsson and B. I. Lundqvist, Phys. Rev. B 13, 4274 (1976).

[20]O. K. Andersen, W. Klose, and H. Nohl, Phys. Rev. B 17, 1209 (1978).

[21]O. Jepsen and O. K. Andersen, Solid State Commun. 9, 1763 (1971).

[22]J. C. Slater, *Quantum Theory of Molecules and Solids* (McGraw-Hill, New York, 1963), Vol. 1.

[23]See, e.g., A. G. Sitenko, *Lectures in Scattering Theory* (Pergamon, New York, 1971).

[24]In all the calculations apart from that of Li, the formula of L. Hedin and B. I. Lundqvist, J. Phys. C 4, 2064 (1971) was used for the non-spin-polarized part of the functional and the spin dependence was obtained from Ref. 19. To be able to compare with the results of Ref. 25 for Li, we have used the full functional of Ref. 19 in the Li calculation.

[25]E. Zaremba, L. M. Sander, H. B. Shore, and J. H. Rose, J. Phys. F 7, 1763 (1977); M. J. Stott and E. Zaremba, Phys. Rev. B 22, 1564 (1980), and private communication.

[26]M. Hamazaki, S. Asano, and J. Yamashita, J. Phys. Soc. Jpn. 41, 378 (1976).